

IMPORTANCE OF ARP3 RESIDUE ARGININE 161 (R161) FOR NEURITE
OUTGROWTH AND THE INTERACTION BETWEEN WAVE1
AND THE ARP2/3 COMPLEX

A THESIS

SUBMITTED IN PARTIAL FULFILLMENT OF THE REQUIREMENTS
FOR THE DEGREE OF MASTER OF SCIENCE
IN THE GRADUATE SCHOOL OF THE
TEXAS WOMAN'S UNIVERSITY

DEPARTMENT OF BIOLOGY
COLLEGE OF ARTS AND SCIENCES

BY

SOUNICK HALDAR M.B.B.S. (M.D.)

DENTON, TEXAS

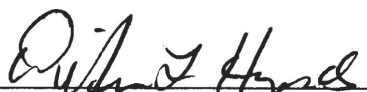
DECEMBER 2012

TEXAS WOMAN'S UNIVERSITY
DENTON, TEXAS

October 23, 2012

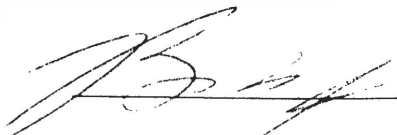
To the Dean of the Graduate School:

I am submitting herewith a thesis written by Sounick Haldar entitled "Importance of Arp3 Residue Arginine 161 (R161) for Neurite Outgrowth and the Interaction between Wave1 and the Arp2/3 Complex". I have examined this thesis for form and content and recommend that it be accepted in partial fulfillment of the requirements for the degree of Master of Science with a major in Biology.



DiAnna Hynds, Ph.D., Major Professor

We have read this thesis and recommend its acceptance:







Department Chair

Accepted:



Dean of the Graduate School

DEDICATION

To my family, Asit Kumar Haldar, Adv. Bharati Haldar, Dr. Ananya Bhattacharya and Dr. Soumendu Bhattacharya, and my friends; without you the entire journey of my life would not have been possible. You are my inspiration and encouragement. Thank you for the endless and selfless love, care and support at each and every stage of my life.

ACKNOWLEDGEMENTS

I would like to express a deep and sincere gratitude to my guide Dr. DiAnna Hynds for her valuable guidance and support that made this research work possible. I am truly and deeply grateful to you for all the encouragement, optimism and confidence.

I would also like to thank my committee members Dr. Lynda Uphouse and Dr. Brian W. Beck for their constant support, guidance and suggestions that helped me throughout the course of the research.

Words are not enough to express my deep sense of appreciation towards my lab mates and friends. I am grateful to God for gifting me with such a precious treasure of friendships. Thanks to all my friends for being my second family.

Thank you Mom and Dad for being the pillars of my life. Thank you for all the prayers, blessings, love, care, encouragement, advice, guidance and the list is never-ending. To my sister and brother-in-law; thank you for being a great support and inspiration. I always value your words of wisdom.

Above all, I would like to thank God for giving me the strength and showering all the blessings.

ABSTRACT

SOUNICK HALDAR

IMPORTANCE OF ARP3 RESIDUE ARGININE 161 (R161) FOR NEURITE OUTGROWTH AND THE INTERACTION BETWEEN WAVE1 AND THE ARP2/3 COMPLEX

DECEMBER 2012

Axon extension results from branched actin nucleation and polymerization leading to lamellipodial expansion. This process is regulated by interaction of the Wiskott-Aldrich syndrome protein (WASP), WASP family verprolin-homologous 1 (WAVE1), with actin binding proteins of the actin related protein (Arp) 2/3 complex. The Arp2/3 complex is composed of seven proteins (Arp2, Arp3 and accessory proteins ARPC1-5) and binds to existing actin filaments to initiate (nucleate) new side chains. Both Arp2 and Arp3 bind to actin filaments; however, the amino acid residues in Arp3 that contribute to this association and interaction of the Arp2/3 complex with WAVE1 are not yet identified. Using computational structure simulations, we predicted that Arp3 arginine 161 (R161) contributes the most to Arp3 interacting with Arp2. To test whether this prediction is true, we have expressed N-terminal green fluorescent protein (GFP)-tagged wild-type and mutant Arp3 (with R161 mutated to alanine) in B35 neuroblastoma cells and determined the effects on Arp2/3 complexing with WAVE1, actin filament content and neurite outgrowth using immunocytochemistry, co-immunoprecipitation and image analysis. Expression of Arp3-R161A in B35 neuroblastoma cells decreased neurite

outgrowth (79.36% decrease in the number of neurite bearing cells) and increased cortical phalloidin staining by 25.74%. Arp2 and WAVE1 co-immunoprecipitated with expressed wild-type Arp3 and Arp3-R161A, providing evidence that the mutant Arp3 participated in the Arp2/3 complex formation, which could still interact with WAVE1. *In vitro*, actin polymerization was increased by extracts from cells expressing the Arp3-R161A gene. We interpret these data to indicate that residue R161 of Arp3 is important for regulating Arp2/3 complex binding to actin filaments and that mutation of this residue to alanine promotes this binding, increasing actin polymerization and decreasing neurite outgrowth. Understanding the mechanisms of Arp2/3 complex function may identify sites for therapeutic action for promoting axon regeneration following traumatic and neurodegenerative lesions.

TABLE OF CONTENTS

	Page
DEDICATION	iii
ACKNOWLEDGMENT.....	iv
ABSTRACT.....	v
LIST OF TABLES.....	ix
LIST OF FIGURES	x
 Chapter	
I. INTRODUCTION.....	1
II. ARP3 RESIDUES IMPORTANT TO THE ARP2/3 FORMATION OF BRANCHED ACTIN FILAMENTS	9
Introduction.....	9
Methods.....	10
Generation of green fluorescent protein (GFP) tagged Arp3.....	10
Site-directed mutagenesis	11
Gel electrophoresis.....	13
Transfection in B35 neuroblastoma cells.....	13
Immunocytochemistry	13
Co-immunoprecipitation.....	14
Actin polymerization assay.....	15
Results.....	16
Generation of Arp3 expression vectors.....	16
Expression of Arp3-R161A alters actin filament arrangement and cell morphology	21
GFP-Arp3-R161A still forms an Arp2/3 complex.....	22
Extracts from cells expressing Arp3-R161A have an increased rate of actin polymerization	23
Discussion.....	24

III. MUTATING ARP3 ARGININE 161 DECREASES NEURITE OUTGROWTH WITHOUT DISRUPTING WAVE1 AND ARP2/3 COMPLEX INTERACTIONS.....	26
Introduction.....	26
Methods.....	27
Immunocytochemistry for co-localization.....	28
Analysis of outgrowth.....	28
Statistics	29
Results.....	30
Expression of Arp3-R161A does not affect binding of other Arp2/3 members to WAVE1	30
Expression of Arp3-R161A decreases neurite outgrowth	32
Expression of Arp3-R161A increases lamellipodial actin filament content	37
Discussion.....	40
IV. FURTHER DISCUSSION.....	44
REFERENCES	50

LIST OF TABLES

Table	Page
3.1. Quantification of lamellipodial phalloidin fluorescence intensity in different treatment groups.	40

LIST OF FIGURES

Figure	Page
1.1. Growth cone at the tip of a growing neurite	2
1.2. Actin filament branch-point.....	5
1.3. Flowchart of the project plan	8
2.1. Plasmid map showing the site for mutation, R161, on Arp3 gene	12
2.2. Restriction digestion of recombinant GFP-Arp3 WT with BglI restriction enzyme.....	18
2.3. Immunocytochemistry of GFP (a,b) and GFP-Arp3(c,d) transfected cells with anti-GFP antibodies (100X).....	19
2.4. Western blot of transfected and untransfected cell extracts.....	20
2.5. Co-immunoprecipitation of WAVE1 from transfected and untransfected cell extracts	21
2.6. Representative 100X images of phalloidin stained untransfected (a) B35 neuroblastoma cells and cells transfected with EV (b), WT (c) and R161A (d) plasmids.....	22
2.7. Co-immunoprecipitation of extracts from untransfected (UT) cells and cells transfected with empty vector (EV: only GFP), wild type Arp3 (WT) and mutant Arp3 (R161A). (a) Co-immunoprecipitated with anti-Arp2 antibodies and blotted with anti-GFP antibodies.....	23
2.8. In-vitro actin polymerization studies of extracts from cells transfected separately with WT and R161A Arp3 gene.....	24
3.1. Co-immunoprecipitation of extracts from untransfected (UT) cells and cells transfected with empty vector (EV: only GFP), wild type Arp3 (WT) and mutant Arp3 (R161A). (a) Co-immunoprecipitated with anti-GFP antibodies and blotted with anti-Arp3 antibodies.....	31

3.2. Co-immunoprecipitation of extracts from untransfected (UT) cells and cells transfected with empty vector (EV: only GFP), wild-type Arp3 (WT) and mutant Arp3 (R161A). (a) Co-immunoprecipitated with anti-Arp2 antibodies and blotted with anti-WAVE1 antibodies.	32
3.3. Immunocytochemistry of untransfected cells (a-e) or cells expressing only GFP (f-j), GFP-Arp3(WT) (k-o), or GFP-Arp3-R161A (R161A; p-t) with anti-GFP antibodies (green), Texas-red phalloidin (red) and DAPI (blue) staining (40X).	33
3.4. Quantification of the percentage of neurite bearing cells in different treatment groups.....	35
3.5. Quantification of the number of neurites per cell in different treatment groups (including only cells with neurites).	35
3.6. Quantification of the number of branches per neurite in different treatment groups.....	36
3.7. Quantification of the neurite length per cell in different treatment groups	36
3.8. Quantification of the longest neurite per cell in different treatment groups.....	37
3.9. Immunocytochemistry of untransfected cells (a-c) or cell transfected with GFP (d-f), GFP-Arp3(WT; g-i), or GFP-Arp3-R161A (R161A; j-l) with anti-GFP antibodies (a,d,g,j,m; green) along with phalloidin (b,e,h,k,n; red) staining (100X).....	38
3.10. Quantification of the cell body phalloidin stain fluorescence intensity in different treatment groups.....	39

CHAPTER I

INTRODUCTION

Injury to the central nervous system (CNS) results in permanent loss of function due, in part, to loss of neurons and appropriate substrata (Lu et al., 2004). While neurons spared following injury have good capacity for regeneration and synaptic plasticity (Alto et al., 2009), an abundance of CNS inhibitors released post-lesion limit axon regeneration (Duo et al., 2009). Proper reinnervation may lead to recovery of function if. However, encouraging sprouting without also ensuring that regenerating axon connect to appropriate targets may result in additional dysfunction. Understanding the molecular mechanisms that promote axon extension may lead to novel therapeutic strategies to encourage axon regeneration after CNS injury.

Axon growth is directed by a sensory motile structure, the growth cone, located at the tip of extending axons. Growth cones are composed of a microtubule-rich central domain and a peripheral domain dominated by actin filaments (Fig. 1.1). In the peripheral domain, actin filaments form two structures, filopodia and lamellipodia. Filopodial and lamellipodial dynamics are regulated by actin polymerization and depolymerization (Aspenstrom et al., 1999; Dickson et al., 2001; Garrity et al., 1999; Luo et al., 1996; Mueller et al., 1999; Nikolic et al., 2002).

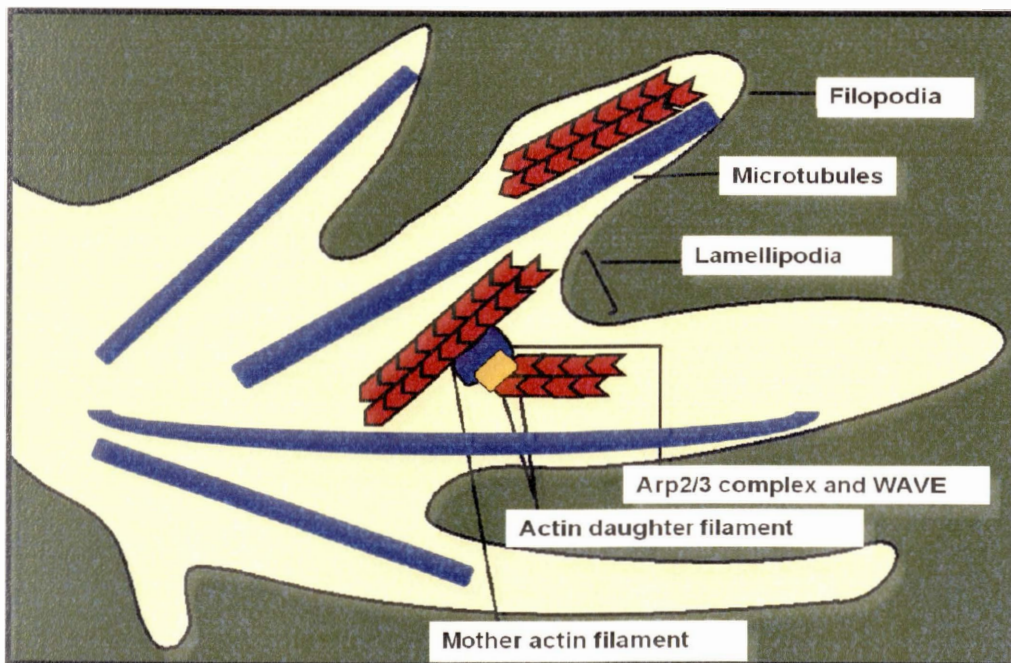


Fig. 1.1: Growth cone at the tip of a growing neurite. The peripheral domain is composed of filopodia, finger like projections made up of cytoskeletal structures primarily composed of linear actin filaments that act as long range sensors, and lamellipodia, broadened areas made up of branched actin filaments responsible for advancing the growth cone. Actin filament branching in lamellipodia is facilitated by WAVE1 activation of the Arp2/3 complex. Adapted from Baas et al., 2001.

Actin shuttles between monomeric and polymeric forms, with polymers producing actin filaments. Actin polymers are directional, having barbed and pointed ends, based on electron microscopy patterns of filaments decorated with the S1 subunit of myosin (Maruyama et al., 1990). In growth cones *in vivo*, the barbed ends are located toward the plasma membrane. The dynamics resulting in changes in actin filaments involve regulated nucleation, polymerization, severing and depolymerization, processes directed by a set of actin binding proteins. Nucleation is the initiation of filaments and

can occur *de novo*, at the end of existing filaments, or from the sides of existing filaments (Rouiller et al., 2008). Profilin binds actin monomers and facilitates nucleotide exchange, promoting polymerization by delivering active monomers to the barbed ends of filaments (Machesky et al., 1994) Cofilin is an actin severing and depolymerizing protein that separates filaments into monomeric actin (Meyer et al., 2002). In addition, capping proteins limit actin filament growth by binding to the barbed ends of actin filaments (Pollard et al., 2003).

Actin filaments may be arranged in linear or branched configurations, based on the method of nucleation and polymerization. Bundles of linearly-arrayed actin filaments form filopodia, whereas lamellipodia have a meshwork of actin filaments. The branched actin filament network observed in growth cone lamellipodia is the result of the actin related protein 2/3 (Arp2/3) complex interaction with Wiskott-Aldrich Syndrome family proteins (WASP), including WASP, neuronal WASP (N-WASP) and verprolin-homologous 1 WASP (WAVE1) proteins (Meyer et al., 2002). The Arp2/3 complex (Machesky et al., 1994) is made up of seven proteins: Arp2, Arp3, ARPC1, ARPC2, ARPC3, ARPC4 and ARPC5 (Rodal et al., 2005; Rouiller et al., 2008; Millard et al., 2004). The complex is inactive by itself but, when activated by a WASP family protein, acts as a nucleator to promote actin branching (Dominguez et al., 2009; Song et al., 2001; DesMarais et al., 2004; Shakir et al., 2008) and lamellipodia formation (Goldberg et al., 2000). At the same time, Arp2/3 complex inhibition or Arp3 knock down results in

similar neuromorphological changes (Pinyol et al., 2007), which might suggest that Arp3 is extremely important for the function of the Arp2/3 complex.

Important to this work is the WASP protein, WAVE1. It and other WASP family members are usually in an auto-inhibited state until Cdc42 or Rac1 disrupts the auto-inhibition, either through direct binding (Cdc42) or through the interaction of intermediate kinases like Pak1, Pak2, Pak3 and myotonic dystrophy kinase-related Cdc42-binding kinases (MRCK; Nikolic et al., 2002; Mullins et al., 2000; Bompard et al., 2004; Padrick et al., 2008; Leung et al., 2008). The COOH-terminus of WAVE1 has a verprolin homology, central sequence and acidic region (VCA) domain, which binds to the Arp2/3 complex to activate it (Wegner et al., 2008). The VCA domain binds to the Arp2/3 complex and actin monomers strongly, without which the actin nucleation is extremely slow (Beltzner et al., 2007).

The molecular structure through which WAVE1 interacts with the Arp2/3 complex has not been completely determined, but understanding the details on how the Arp2/3 complex nucleates actin polymerization may provide a target for new therapeutics to encourage axon growth. Thus, it is essential to elucidate this mechanism of action. Arp2 and Arp3 are actin homologs (Rodal et al., 2005). The other five subunits of the Arp2/3 complex provide for integrity of the complex, while maintaining a distance between Arp2 and Arp3 that prevents nucleation until the complex is activated by a WASP family protein (Beltzner et al., 2007). When associated with a WASP family protein, the Arp2/3 can bind adenosine triphosphate (ATP), changing its quaternary

conformation to place the complex in an active state with its nucleotide binding cleft in a closed conformation (Kiselar et al., 2006). The activated complex binds to an existing actin filament to form a base for the formation of a new actin polymer at a 70° angle to the existing filament (Rouiller et al., 2008) (Fig. 1.2). This leads to the branching of actin filaments (Rodal et al., 2005; Rouiller et al., 2008). However, the function of nucleotide binding to the Arp2/3 complex is not entirely clear. Dayel et al. (2001) claim that hydrolysis of bound ATP is needed for activation of the nucleating capacity of the Arp2/3 complex.

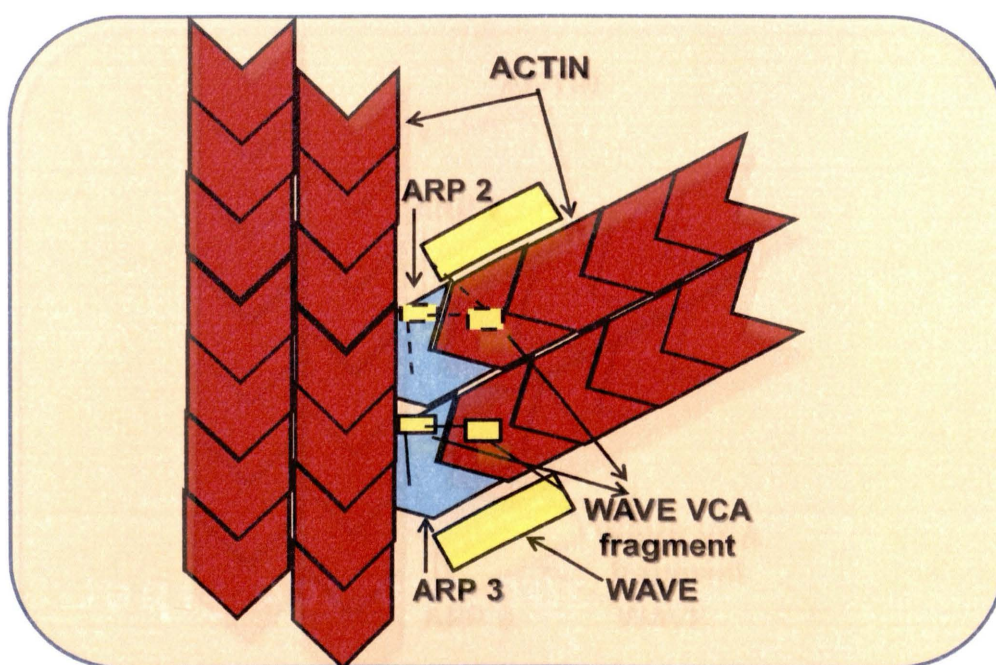


Fig. 1.2: Actin filament branch-point. The WAVE-Arp2/3 complex binds to the sides of mother actin filaments to initiate branch formation. The daughter filament grows with Arp2/3 complex as its foundation. Adapted from Dominguez et al., 2009.

It is well known that the Arp2/3 complex is activated by WASP proteins, including WAVE1 (Boczkowska et al., 2008; Seifert et al., 2008). However, it is not clear whether WAVE1 binds to Arp3 alone or to Arp3 and Arp2 simultaneously for activation of the complex. An X-ray scattering study of activated Arp2/3 complex bound to actin and a single molecule of WAVE1 suggests that the central sequence motif of WAVE1 binds to the Arp2 subunit and the acidic region motif of WAVE1 binds to Arp3 subunit of Arp2/3 complex (Boczkowska et al., 2008). This can imply that the Arp3-Arp2 interface is regulated by interaction with WAVE1, with WAVE1 potentially directing an interfacial conformation change between Arp2 and Arp3. However, another study suggests that a dimer of the VCA domains of WAVE1 binds to the Arp2/3 complex more readily than a WAVE1 monomer (Padrick et al., 2008). According to Rodal et al. (2005) binding of a WASP protein to the Arp2/3 complex brings Arp2 and Arp3 into closer structural contact to facilitate binding to the actin mother filament. The interaction between WASP proteins and the Arp2/3 complex appears to depend primarily on interaction with Arp3, as Arp2 does not have high affinity for the VCA domain of WAVE1 (Nolen et al., 2008). Thus, investigating how WAVE1 regulates the interface between Arp2 and Arp3 may provide mechanistic clues on the regulation of lamellipodia formation and axon growth.

We are able to use computational protein structure calculations to determine the residues in the interface between Arp2 and Arp3 that contribute the most towards the function of Arp3. Computational studies performed by Amruta Mahadik and colleagues

(Mahadik et al., in preparation) using Kortemme and Baker alanine scans (Kortemme et al., 2004) and Lichtarge's evolutionary tracing (Lichtarge et al., 1996) predicted three Arp3 residues that likely contribute a lot towards the Arp3-Arp2 interface: arginine 161 (R161), serine 226 (S226) and arginine 447 (R447). Of these, R161 has the maximum change in the free energy when virtually mutated to alanine, suggesting it is an essential residue for the interface (Mahadik et al., in preparation). If this is true, mutating Arp3 R161 should affect advancement of the growth cone and elongation of the neurite, a question addressed by performing the studies described herein. In particular, we mutated the Arp3 residue R161 to alanine and expressed mutant and wild-type Arp3 in B35 rat neuroblastoma cells. We then assessed the interaction of WAVE1 with the Arp2/3 complex, as well as lamellipodia formation, lamellipodial actin filament content and neurite extension (Fig. 1.3).

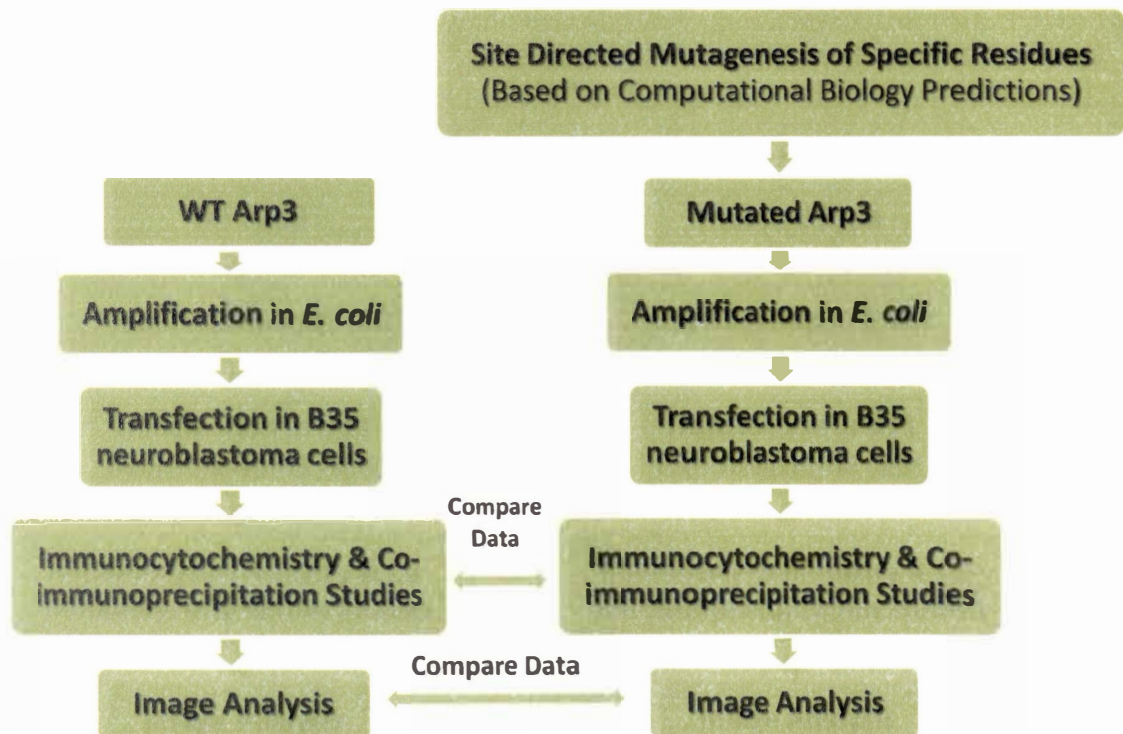


Fig. 1.3: Flowchart of the project plan. Site directed mutagenesis of the important residue in the recombinant DNA was followed by amplification of the WT and mutant Arp3 in *E. coli* and transfected into separate B35 neuroblastoma cells. Changes in the morphology of the cells and WAVE1-Arp2/3 complex interactions were studied with image analysis, immunocytochemistry and co-immunoprecipitation by comparing the WT to the mutant cells.

CHAPTER II

ARP3 RESIDUES IMPORTANT TO THE ARP2/3 FORMATION OF BRANCHED ACTIN FILAMENTS

Excerpts adapted from a manuscript by A.C. Mahadik, , S. Haldar, , D.L. Hynds, , and B.W. Beck, to be submitted to Biophysical Journal

INTRODUCTION

Outgrowth of axons from neurons is the result of lamellipodial expansion at the leading edge of growth cones located at the tips of extending axons (Korobova et.al., 2008). Actin filaments in lamellipodia are arranged in a branching network. The polymerization and branching of actin filaments are further dependent on various proteins, including Arp3 of Arp2/3 complex. Through virtual alanine scans and evolutionary tracing Arp3, we predicted residue arginine 161 (R161) to have the largest contribution for the interface between Arp2 and Arp3. In particular, the computational simulations were conducted using a structure without a bound nucleotide, so the complex was in an open conformation cleft or functionally inactive structure.

Since actin polymerization and organization is important for growth cone extension and axon branching (Schmidt et al., 2010), we planned to analyze the effect of expressing Arp3 with an arginine to alanine mutation at residue R161 (R161A) on neurite initiation and outgrowth. Here, we have developed expression vectors containing wild-

type Arp3 and Arp3-R161A. We tested the effect of R161A on actin polymerization *in vitro* and *in vivo*.

METHODS

The protocols for virtual alanine scan (VAS), comparison of full length cDNA, evolutionary trace (ET) and multi sequence alignment are described in detail in a manuscript produced from this project (Mahadik et al., in preparation). Here, we describe the methods used to construct the vectors used in this study and the bench experiments testing the results of the computer simulation experiments.

Generation of green fluorescent protein (GFP) tagged Arp3

A GFP-tagged Arp3 construct was generated to facilitate the identification of transfected cells. This required amplification of two plasmids: an entry vector containing the complete open reading frame (ORF) of human Arp3 (1373 bp); and a destination vector containing GFP (717 bp), V5 epitope (42 bp), chloramphenicol resistance (Chlor^r) and ampicillin resistance (Ampr^r) genes (N-EmGFP-DEST, Invitrogen). Each vector was first amplified in One Shot Top 10 cells (*E. coli*) cultured in Lysogeny broth (LB; Bertani et al., 1951) with appropriate selection (spectinomycin resistance for entry vector, chloramphenicol resistance for destination vector). Plasmid DNA was isolated using Qiagen Miniprep and Midiprep kits.

To generate GFP-tagged Arp3, the ORF was transferred into the destination vector by homologous recombination with LR Clonase II (Invitrogen, Carlsbad, CA) in Tris/EDTA. This enzyme cuts each vector at specific sites and facilitates the exchange of Arp3 in the entry vector with the chloramphenicol resistance gene in the destination vector. The final construct produced had the genes for GFP and V5 epitope attached to the two ends of the Arp3 gene with linkers of 15 bp and 7 bp respectively. *E.coli* transformed with the recombinant DNA was grown in LB medium plates with ampicillin (100µg/ml) (Sigma, St. Louis, MO). Recombinants were selected based on ampicillin resistance (demonstrating presence of plasmid) and chloramphenicol sensitivity (indicating recombination). In each case transformation efficiencies were estimated using the control plasmid pUC19. Restriction digestion with BglI and sequencing were used to confirm correct recombination.

Site-directed mutagenesis

Computational modeling of actin, Arp2/3 and WAVE1 protein interactions using evolutionary trace and virtual alanine scanning identified R161 as contributing the highest energy interaction at the Arp2/Arp3 interface. Site directed mutagenesis was done with QuickChange II Site-Directed Mutagenesis Kit (Invitrogen, Carlsbad, CA), according to the manufacturer's suggestions. Primers used to mutate R161 to alanine were sense: 5'- CTCCACTCA ATACACCAGAAA ACGCAGAGTATCTTGCAG AAATTATGT -3' and antisense: 5'- ACATAATTTCTGCAAGATACTCTGCGTTTTTC

TGGTGTATTGAGTGGAG -3' (red text indicates site of mutation). Both primers were used in polymerase chain reaction (PCR)-based generation of mutated Arp3. The initial PCR program was 16 thermal cyclings with the following steps: (1) 95°C for 30 sec for melting; (2) 55°C for 1 min for annealing; and (3) 68°C for 7 min for elongation. DpnI was used to digest the parental dsDNA. Mutation was verified by sequencing (Biosynthesis). A map of the expression vector containing mutated Arp3 is shown in Fig. 2.1)

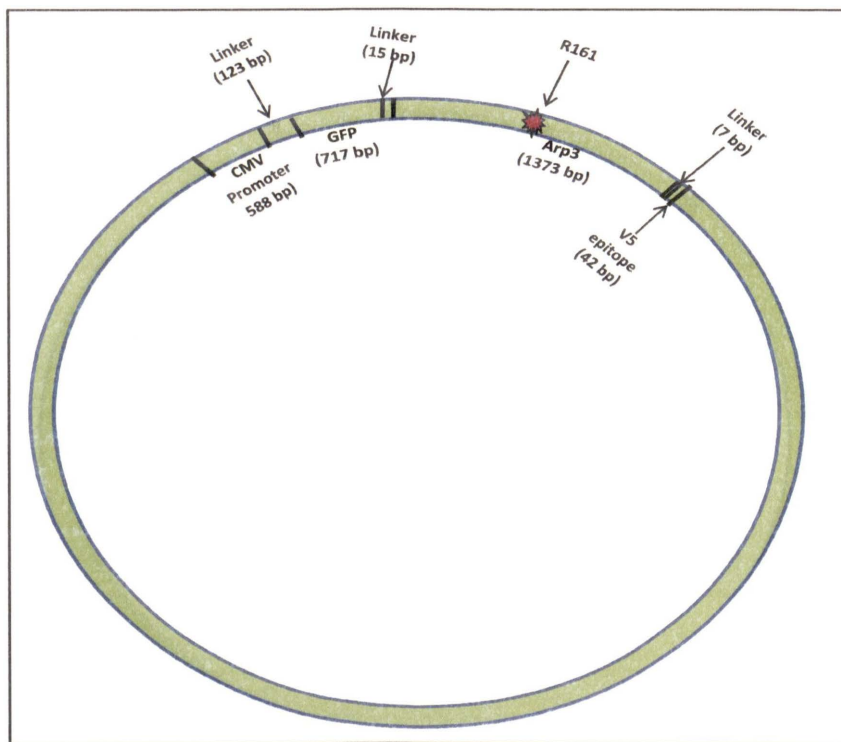


Fig.2.1. Plasmid map showing the site for mutation, R161, on Arp3 gene. GFP and V5 epitope are attached to the two ends of Arp3 with linkers.

Gel electrophoresis

Gel electrophoresis was done to confirm the sizes of the DNA and its fragments after restriction digestion. Samples were mixed 1:1 with loading buffer (bromophenol blue) and electrophoresed through 1.5% agarose gels in Tris-Acetate-EDTA (TAE) buffer for 1 hour at 130 V. DNA was labeled with 25 mg/ml ethidium bromide for 30 min and the size of DNA fragments were compared to a standard DNA ladder.

Transfection in B35 neuroblastoma cells

B35 rat neuroblastoma cells were used for the expression of the wild-type and mutant Arp3. These cells were routinely cultured in 10% fetal bovine serum (FBS)-containing medium and incubated at 37°C until 90% confluent. For splitting cells, 0.25% trypsin in phosphate buffered saline (PBS) was used. For biochemical experiments (co-immunoprecipitation and western blot), cells were seeded in 6-well plates at a density of 20,000 cells/cm². Lipofectamine™ 2000 was used to transfect B35 rat neuroblastoma cells according to manufacturer's instructions.

Immunocytochemistry

Transfection efficiencies were estimated using immunocytochemistry for GFP. For immunocytochemistry experiments, cells were seeded in 6-well plates at a density of 10,000 cells/cm². Controls included untransfected cells and cells transfected with empty vector (vector with GFP but no Arp3). Two days after transfection, the cells were fixed in

4% paraformaldehyde and immunolabeled with mouse anti-V5 (1:200; Invitrogen, Carlsbad, CA) and rabbit anti-GFP (1:200; Invitrogen, Carlsbad, CA) antibodies. V5 is an additional tag located at the C terminus of the Arp3 gene. Immunolabeling was visualized using appropriate secondary antibodies including Alexafluor 488-conjugated goat anti-mouse and Alexafluor-555 conjugated donkey anti-rabbit antibodies (Invitrogen, Carlsbad, CA). Actin was stained with Texas Red-phalloidin (165 nM; Invitrogen, Carlsbad, CA). One image per replicate (3 per condition) was captured with 40X and 100X objectives. Transfection efficiencies were estimated by comparing the number of cells expressing GFP to the total number of cells in each image.

Co-immunoprecipitation

Co-immunoprecipitation and western blot studies were done to determine the extent that WAVE1 associates with Arp3 in B35 cells that remained untransfected as well as in cells transfected with empty vector (EV; GFP alone), GFP-wild type (WT) Arp3 or GFP-R161A Arp3. Cell lysates (400 μ g total protein) were precipitated overnight at 4°C with rabbit anti-WAVE1 antibodies (10 μ g) and incubated with protein A agarose beads for 2 hrs at room temperature. Immunoprecipitates and lysates were electrophoresed through 12% sodium dodecyl sulfate polyacrylamide gels (SDS-PAGE) and transferred to nitrocellulose. Nitrocellulose was blocked in 5% nonfat dry milk in Tris buffered saline containing 0.1% Tween-20 (TBST). Blots were probed with rabbit anti-GFP antibodies (1:1000) overnight followed by goat anti-rabbit antibodies conjugated to horse

radish peroxidase (1:5000) for 2 hours and immunoreactive bands were visualized by enhanced chemiluminescence and were quantified using scanning densitometry readings. The nitrocellulose was stripped and re-probed with anti-Arp3 (to confirm WAVE1/Arp3 complexing), anti-Arp2 (to determine Arp3 R161 interruption of Arp3/Arp2 complexing) and anti-WAVE1 antibodies (to evaluate the efficiency of the immunoprecipitation). The experimental controls were anti-WAVE1 antibody precipitates of lysates from untransfected and GFP-only cultures; and the negative control for immunoprecipitation was normal rabbit serum precipitates. In addition, reverse immunoprecipitations with anti-GFP or anti-Arp3 antibodies were performed.

Actin polymerization assay

Actin Polymerization Biochem Kit (Cytoskeleton, Denver, CO) was used to measure actin polymerization rates in B35 cells that remained untransfected as well as in cells transfected with EV, GFP-WT Arp3 or GFP-R161A Arp3. In this assay, increased polymerization is measured by increased fluorescence from pyrene-conjugated actin. Lysates from cells transfected with WT and R161A Arp3 were incubated with pyrene-conjugated G-actin (0.4 mg/ml) in the presence of ATP and the samples were read with a fluorimeter (Tecan). The samples were read at 60 second intervals for 20 minutes without actin polymerization buffer (APB) and for 1 hour after the addition of APB. Baseline controls only had ATP and General Actin Buffer. Spontaneous actin polymerization for each treatment condition (at time = 1 min) was subtracted from each group (baseline

control, test buffer/positive control, wild-type samples and mutant samples). The pyrene label minimally affects the rate of actin polymerization.

RESULTS

The virtual alanine scan of Arp3 subunit of Arp2/3 complex in the open state revealed one strong hot spot ($\Delta\Delta G_{\text{subst}} > 2$ kcal/mol) at R161 and two moderate hot spots ($\Delta\Delta G_{\text{subst}} > 1$ kcal/mol but less than 2 kcal/mol) at S226 and R447 in Arp3. The highest free energy change was seen with substituting alanine for arginine at residue 161, with a 3.98 kcal/mol free energy change. R161 was also shown to be energetically important in the intermediate and closed states defined here as having a free energy change of more than 1 kcal/mol after its substitution with alanine (data not shown). Thus, R161 was predicted to have the largest energy contribution to the interface between Arp2 and Arp3.

Generation of Arp3 expression vectors:

To determine the contribution of R161 in Arp3 in regulating actin nucleation, we generated expression vectors containing Arp3 N-terminally fused to GFP. Restriction digestion of GFP-Arp3 WT recombinant vector with BglI restriction enzyme produced three fragments of roughly 4000kb, 1800kb and 1200kb sizes (fig. 2.2) suggesting that the homologous recombination generated the proper recombinant DNA since one of the restriction sites (needed for a total of three fragments) was within the insert. When B35 neuroblastoma cells were transfected with GFP-Arp3, immunocytochemistry for GFP

indicated that nearly 100% of the cells were transfected with either empty vector or with GFP-Arp3 (fig. 2.3). The cells were viable in all the groups 3 days after transfection indicating minimal toxicity due to the transfection method and protocol. In western blotting experiments, anti-GFP immunoreactive bands were found at 75 kDa (the expected molecular weight of the fusion protein) in transfected cells, but not in untransfected cells (fig. 2.4a). Furthermore, anti-Arp3 western blots had immunoreactive bands at 50 kDa in both transfected and untransfected cells, corresponding to the expected molecular weight of endogenous Arp3 (fig. 2.4b). An additional Arp3 immunoreactive band was also evident at approximately 75 kDa (the expected size of the fusion protein) in transfected, but not in untransfected cells (fig. 2.4b).

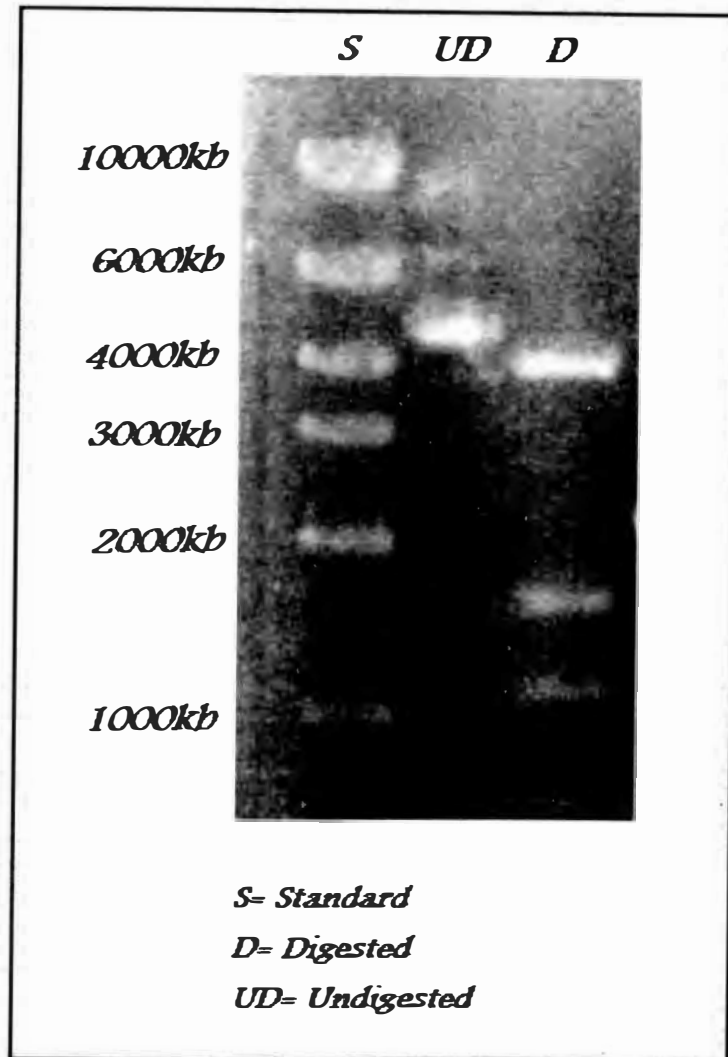


Fig. 2.2: Restriction digestion of recombinant GFP-Arp3 WT with BglI restriction enzyme. 1.5% agarose gel electrophoresis was done to separate the fragments. The digest pattern with bands at 4000, 1800 and 1200 bp suggested that the vector contained Arp3 in the correct orientation.

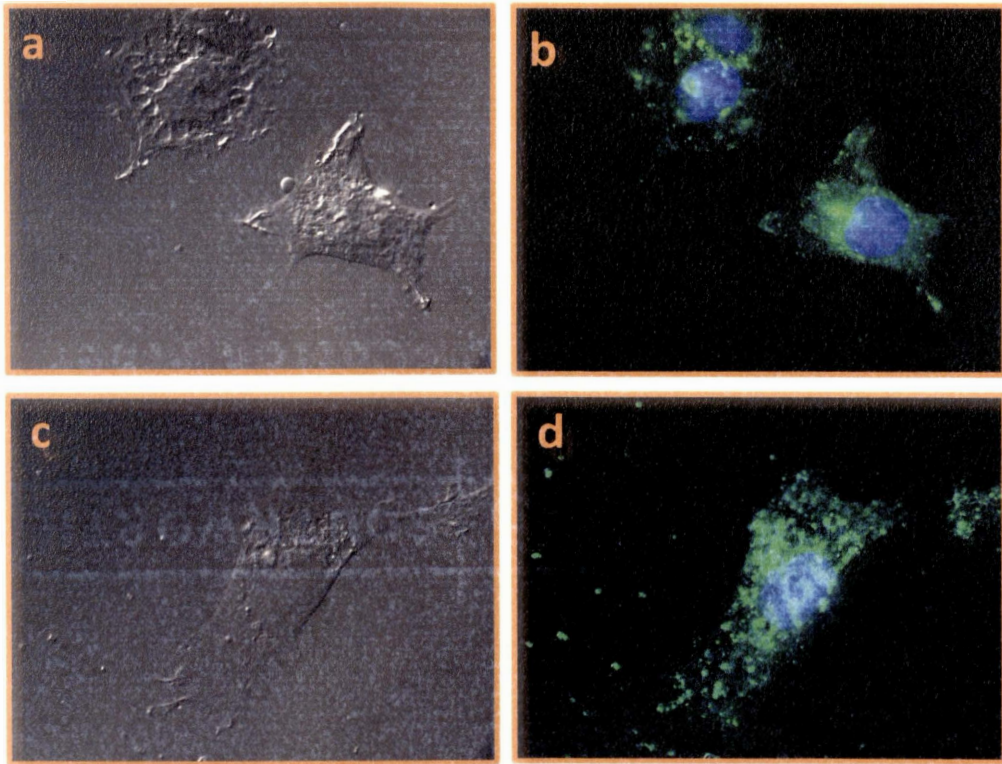


Fig. 2.3. Immunocytochemistry of GFP (a,b) and GFP-Arp3(c,d) transfected cells with anti-GFP antibodies (100X). Pictures a and c are the differential interference contrast (DIC), whereas b and d, are the fluorescent images showing the expression of GFP and GFP-Arp3 proteins. The blue color is due to DAPI, which stains the nuclei. The cells are viable and of normal morphology with neurites.

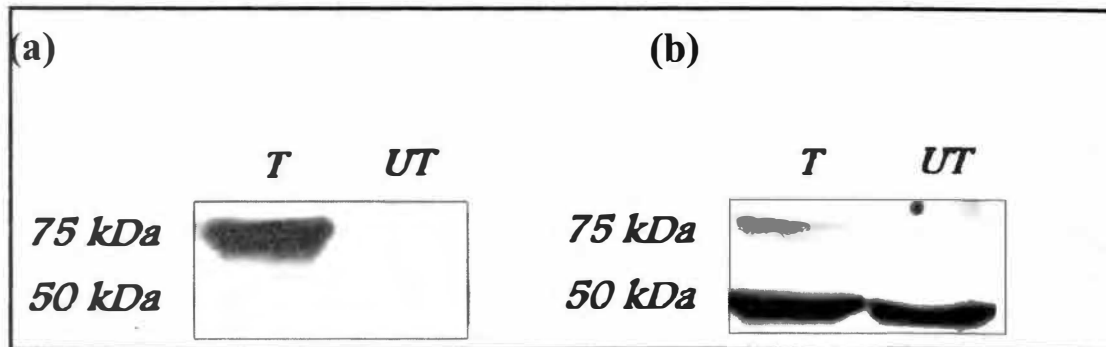


Fig.2.4. Western blot of transfected and untransfected cell extracts. (a) Western blot with anti-GFP antibodies. The lane from cells transfected with GFP-Arp3 shows a band of 75 kDa. (b) Western blot with anti-Arp3 antibodies. The lane from cells transfected with GFP-Arp3 shows a band of 75 kDa, whereas at 50 kDa, bands of endogenous Arp3 are present in both lanes. T=Transfected, UT= Untransfected.

In addition, the expressed Arp3 is capable of interacting with one of its activating proteins, WAVE1. Co-immunoprecipitation of WAVE1 and blotting with anti-GFP antibody (fig. 2.5a) and anti-Arp3 antibody (fig. 2.5b) produced bands of 75 kDa in the lane with extracts from cells transfected with GFP-Arp3 recombinant DNA, suggesting that the GFP-Arp3 chimeric protein is binding with WAVE1. Blotting with anti-Arp3 antibody also produced bands of 50 kDa in both transfected and untransfected lanes because of endogenous Arp3 bound to WAVE1.

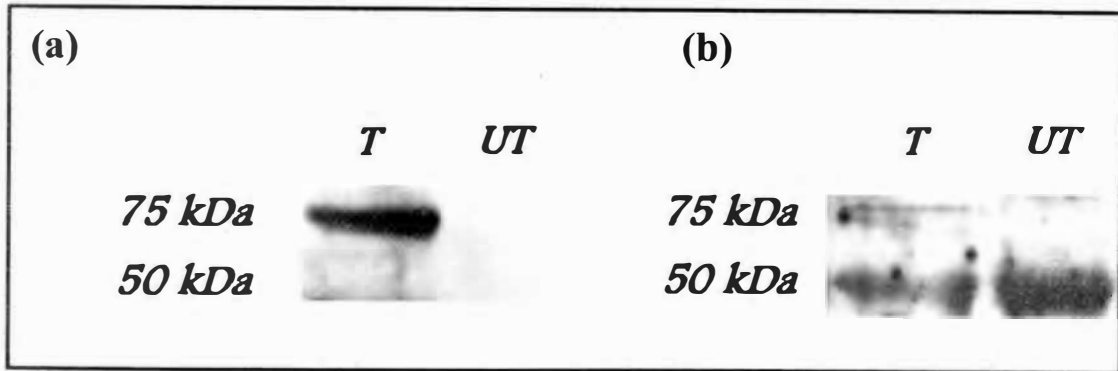


Fig.2.5. Co-immunoprecipitation of WAVE1 from transfected and untransfected cell extracts. (a) Western blot with anti GFP antibodies. The lane from cells transfected with GFP-Arp3 shows a band of 75 kDa. (b) Western blot with anti-Arp3 antibodies. The lane from cells transfected with GFP-Arp3 shows a band of 75 kDa, whereas at 50 kDa, bands of endogenous Arp3 are present in both lanes. T=Transfected, UT= Untransfected.

Expression of Arp3-R161A alters actin filament arrangement and cell morphology:

Following site-directed mutagenesis to generate expression vectors carrying GFP-Arp3 with R161 mutated to alanine, neuroblastoma cells were transfected with wild-type or mutant Arp3. Cells transfected with R161A Arp3 displayed altered cell morphology compared to those transfected with wild-type Arp3 (Fig. 2.6). The cells expressing Arp3-R161A elaborated few if any neurites and had apparently increased accumulation of filamentous actin at the cell cortex. Empty vector (EV; cells transfected with GFP only) and untransfected (UT) groups were used as controls.

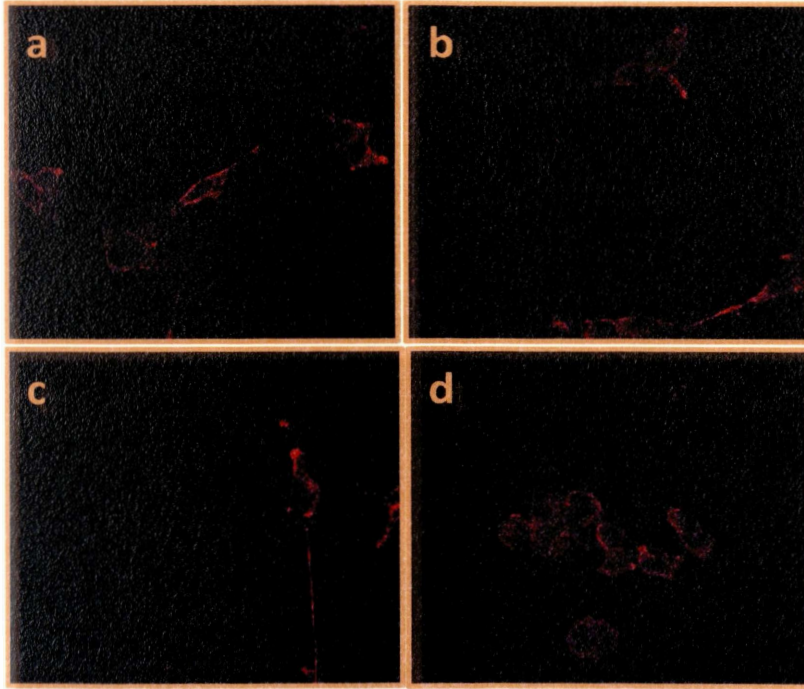


Fig. 2.6. Representative 100X images of phalloidin stained untransfected (a) B35 neuroblastoma cells and cells transfected with EV (b), WT (c) and R161A (d) plasmids.

GFP-Arp3-R161A still forms an Arp2/3 complex:

We next tested whether GFP-Arp3-R161A was able to form an Arp2/3 complex. Extracts of cells transfected with either wild-type or mutant Arp3 were co-immunoprecipitated with anti-Arp2 antibodies. Blotting with anti-GFP antibodies showed 75 KDa bands of similar thickness in the wild-type and R161A lanes, whereas these bands were absent in untransfected cells or cells transfected with GFP only (Fig. 2.7). Similar results were seen with reciprocal co-immunoprecipitations (data not shown). This suggests that Arp3 with the R161A mutation is able to complex with other members of the Arp2/3 complex.

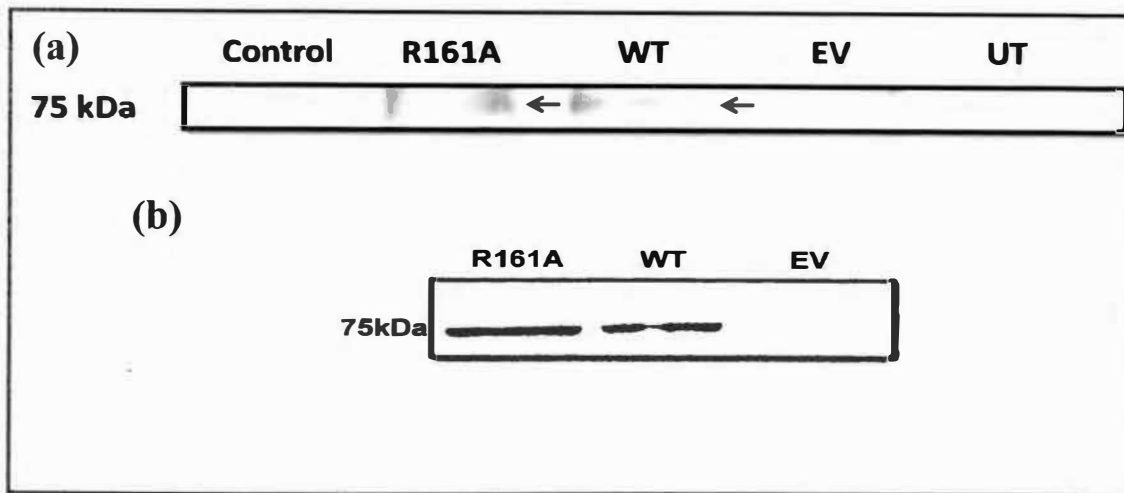


Fig. 2.7. Co-immunoprecipitation of extracts from untransfected (UT) cells and cells transfected with empty vector (EV: only GFP), wild type Arp3 (WT) and mutant Arp3 (R161A). (a) Co-immunoprecipitated with anti-Arp2 antibodies and blotted with anti-GFP antibodies. Bands 75 kDa are present in the WT and R161A lanes. (b) Input blot. Blots are representative of three separate experiments, all of which showed similar results.

Extracts from cells expressing Arp3-R161A have an increased rate of actin polymerization:

Extracts from cells transfected with R161A Arp3 gene showed an increase in the actin polymerization *in-vitro* as compared to that from cells transfected with wild-type Arp3 (Fig. 2.8). Slopes calculated for the linear portion of each curve (5-15 minutes) showed an increase in the actin polymerization rate for extracts of cells expression Arp3-R161A, compared to that of extracts from cells expressing wild type Arp3 or the assay positive control.

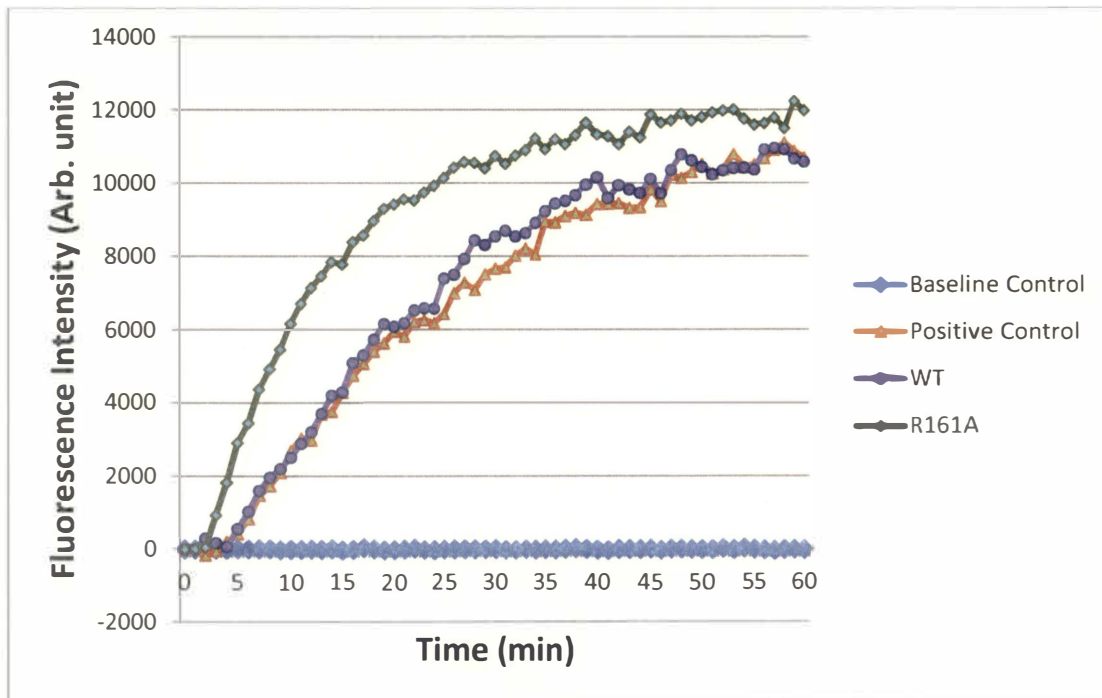


Fig. 2.8. In-vitro actin polymerization studies of extracts from cells transfected separately with WT and R161A Arp3 gene. The experiments were conducted in duplicate and repeated three times. Comparison of the slopes of the linear portion of each curve (between 5 and 15 minutes) indicates that the rate of polymerization is significantly higher in cells expressing Arp3-R161A, compared to cells expressing WT ARP3 at $p < 0.05$ (ANCOVA with LSD post-hoc). This is from a representative experiment.

DISCUSSION

In this work, we identified three Arp3 residues likely to contribute to the Arp2/Arp3 interface (Mahadik et al, in preparation). We constructed vectors to express wild-type and Arp3-R161A in mammalian cells. Both wild-type and mutant Arp3 were able to interact with Arp2. However, expression of Arp3-R161A increased the rate of actin polymerization, with filaments accumulating at the cell cortex and significantly altering cell morphology. The calculations indicating that R161 is an important residue

for the Arp2/3 interface suggested that mutating this residue could either increase or decrease the activity of the Arp2/3 complex. We initially hypothesized that the Arp3-R161A would not be able to interact efficiently with Arp2, subsequently decreasing actin branching and polymerization. This would lead to inability to form lamellipodia and decrease neurite outgrowth. However, we found that the R161A mutation increased actin polymerization, supporting the alternate hypothesis that this mutation would increase activity of the Arp2/3 complex. The increased actin polymerization and accumulation in cells suggests that the mutation made the Arp2/3 complex more efficient. It is likely that the unusually high amount of actin polymerization hinders extension of cellular processes.

Prior work indicates that there may be an optimal level of Arp2/3 activity leading to typical cellular functions. For instance, inactivating Arp2/3 function inhibits actin branch formation and polymerization leading to abnormal actin dynamics, cell motility and endocytosis in some cell lines (Liu et al, 2011). Conversely, studies have shown that increased Arp2/3 complex activity and actin polymerization disrupts many cellular functions leading to binucleated cells, abnormal mitosis, defective cytokinesis and even apoptosis due to unusual localization of actin (Moulding et al, 2007). From the data reported here, we conclude that Arp3 R161 does contribute to the proper functioning of the Arp2/3 complex and mutating this residue to alanine leads to a shift in equilibrium from inactive to active actin branching and polymerization system altering cell morphology in B35 neuroblastoma cells.

CHAPTER III

MUTATING ARP3 ARGININE 161 DECREASES NEURITE OUTGROWTH WITHOUT DISRUPTING WAVE1 AND ARP2/3 COMPLEX INTERACTIONS

Adapted from a manuscript by S. Haldar , A.C. Mahadik, B.W. Beck, and D.L. Hyndsto
be submitted to Journal of Neurobiology

INTRODUCTION

Axon growth during development, regeneration and plasticity of neurons results from extension of a sensory motile structure, the growth cone, located at the tips of extending axons. Forward extension of growth cones requires expansion of peripheral domain lamellipodia, structures containing an actin filament meshwork (Korobova et al., 2008). In particular, nucleation and polymerization of actin near the leading plasma membrane of an extending growth cone is important for axon extension, a process regulated by the actin related protein 2/3 (Arp2/3) complex (Machesky et al., 1994; Aspenstrom et al., 1999; Dickson et al., 2001; Garrity et al., 1999).

The Arp2/3 complex is composed of seven subunits with the Arp2 and Arp3 heterodimer binding to the mother actin filament to nucleate a branching daughter filament (Rodal et al., 2005; Rouiller et al., 2008). The other five subunits provide for integrity of the Arp2/3 complex and maintain the complex in an inactive state incapable

of binding to the mother filament (Beltzner et al., 2008). When the closed form of the Arp2/3 complex interacts with activating WASP family proteins, it adopts an “open,” activated form that can interact with the mother actin filament (Wegner et al., 2008; Nikolic et al., 2002).

The verprolin (V) homology, central (C) sequence and acidic (A) region (VCA) domain of WAVE1 binds to the Arp2/3 complex and actin monomers, aiding in the nucleation process (Beltzner et al., 2007). The VCA domain does not have high affinity for Arp2, suggesting that WAVE1 interaction with Arp3 is important for the nucleation process (Nolen et al., 2008). Other work suggests that the C sequence of WAVE1 binds to Arp2 and the A region to Arp3 (Boczkowska et al., 2008). It is possible that a change in the interface between Arp2 and Arp3 might affect the interaction between WAVE1 and Arp2/3 complex, thus affecting actin nucleation and polymerization. Deciphering the particular molecular interactions that regulate Arp2/3 nucleation and subsequent lamellipodia formation may identify novel therapeutic targets for encouraging axon growth.

METHODS

The protocols for generation of GFP tagged Arp3, site-directed mutagenesis, gel electrophoresis, transfection in B35 neuroblastoma cells, co-immunoprecipitation and

actin polymerization assay have been described in detail in Chapter II. Other methods used are as follows.

Immunocytochemistry for co-localization

Immunocytochemistry was performed using anti-WAVE1 (1:200; Sigma, St. Louis, MO), anti-GFP (1:200; Sigma, St. Louis, MO) and anti-Arp3 (1:200; Sigma, St. Louis, MO) antibodies, and the immunolabeling was visualized with secondary antibodies (1:200) conjugated to Alexafluor 488, Alexafluor 555 or Alexafluor 649. Controls were untransfected cells and cells transfected with GFP only. Treatment groups for these experiments included untransfected control, and cells transfected with GFP only, wild-type Arp3 and mutant Arp3.

Analysis of outgrowth

Neurite outgrowth and actin filament content were analyzed using image analysis of phase contrast and fluorescent images. Cells were stained with Texas Red-phalloidin (165 nM in PBS) to analyze the actin filament content. Digital images were captured through 40X and 100X objectives for quantification of lamellipodia formation, actin filament content and neurite outgrowth. For quantification of lamellipodia formation, areas in the growth cone with characteristic lamellipodial morphology and phalloidin labeling intensity 50% higher than growth cone central regions were defined as lamellipodia and outlined. Phalloidin labeling intensity in the cortical regions of the cell

bodies and lamellipodial regions of the growth cones was used to quantify actin filament content. For neurite outgrowth analysis, the percentage of neurite bearing cells, number of neurites per cell, total neurite length per cell (sum of all processes), the length of the longest neurite for each cell and number of branches per neurite were assessed. Treatment groups for these experiments included untransfected control, GFP only, wild-type and mutant Arp3. Each group was assessed using triplicate cultures in at least 3 separate experiments (n = 9). One image was taken per condition per replica.

Statistics

All end-point assays for the lamellipodia formation, actin filament content and neurite outgrowth yielded normally distributed data with similar variances across experimental groups. The experimental groups were individual cultures expressing wild-type and mutant Arp3, whereas the control groups were untransfected cultures and cultures expressing only the GFP construct. Data were analyzed using univariate analysis of variance (ANOVA) with individual treatment groups as the independent variable and the morphological characteristics as the dependent variable. Differences between treatment groups were determined using the Least Significant Difference (LSD) post-hoc test at the 0.05 level of significance.

RESULTS

Expression of Arp3-R161A does not affect binding of other Arp2/3 members to WAVE1

We assessed whether mutating residue arginine 161 in Arp3 prevents interaction with its activator, WAVE1, using co-immunoprecipitation. GFP immunoprecipitates from cell extracts of cells expressing wild-type or mutant Arp3 had Arp3 immunoreactive bands at approximately 75 kDa (the expected molecular weight of the GFP fusion proteins), whereas untransfected cells or cells transfected with empty vector did not have these immunoreactive bands, suggesting that these two categories of cells expressed the GFP-Arp3 chimeric proteins (Fig.3.1). Negative control immunoprecipitations with normal rabbit serum confirmed successful immunoprecipitation and reciprocal immunoprecipitations yielded similar results (data not shown). The lane of extracts from cells expressing mutant Arp3, however, showed increased Arp3 immunoreactivity, perhaps indicating an effect of the mutation on the efficacy of Arp3-antibody binding or increased production of the mutant compared to cells expressing the wild-type construct. When extracts of cells transfected with either wild-type or mutant Arp3 were co-immunoprecipitated with anti-Arp2 and blotted for WAVE1, immunoreactive bands of approximately 62 kDa with similar thickness were observed in the untransfected, empty vector, wild-type and mutant lanes, but not in cell extracts immunoprecipitated with normal rabbit serum (Fig. 3.2). Similar results were seen with reciprocal co-immunoprecipitations. Together these data suggest that the fusion proteins are being expressed and can be precipitated, and the interaction of other members of the Arp2/3

complex to one of the WASP family activating proteins is not affected by the Arp3 mutation.

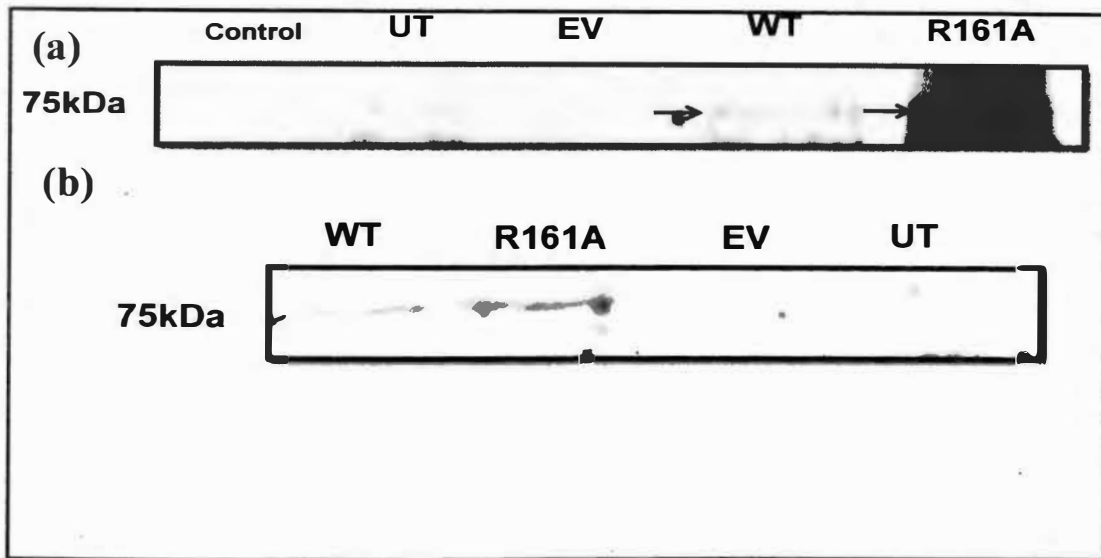


Fig. 3.1. Co-immunoprecipitation of extracts from untransfected (UT) cells and cells transfected with empty vector (EV: only GFP), wild type Arp3 (WT) and mutant Arp3 (R161A). (a) Co-immunoprecipitated with anti-GFP antibodies and blotted with anti-Arp3 antibodies. Bands 75 kDa are present in the WT and R161A lanes. (b) Input blot. Blots are representative of three separate experiments, all of which showed similar results.

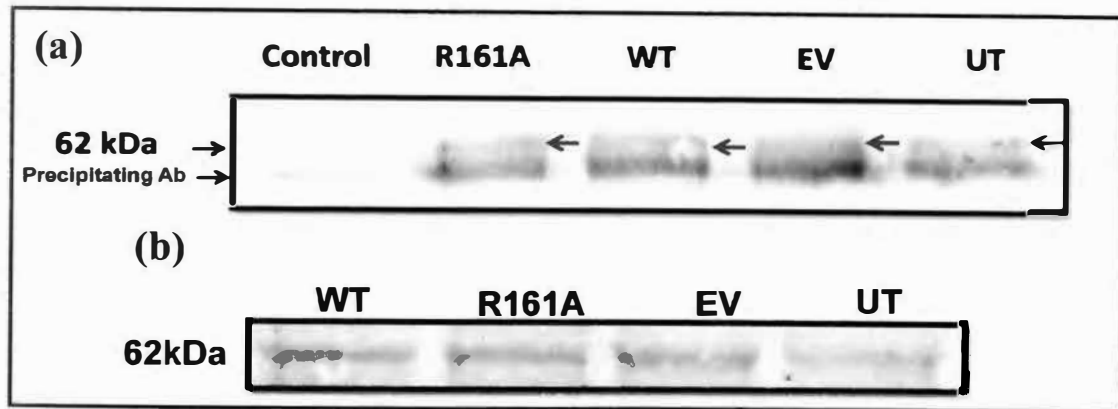


Fig. 3.2. Co-immunoprecipitation of extracts from untransfected (UT) cells and cells transfected with empty vector (EV: only GFP), wild-type Arp3 (WT) and mutant Arp3 (R161A). (a) Co-immunoprecipitated with anti-Arp2 antibodies and blotted with anti-WAVE1 antibodies. Bands of 62 kDa are present in the UT, EV, WT and R161A lanes. (b) Input blot. Blots are representative of three separate experiments, all of which showed similar results.

Expression of Arp3-R161A decreases neurite outgrowth

We used image analysis to assess how expressing wild-type or mutant Arp3 in B35 cells affects neurite outgrowth. Immunocytochemical images of untransfected cells (Fig. 3.3 a-e) and cells transfected with GFP only (Fig. 3.4 f-j), GFP-Arp3 (WT; Fig. 3.4 k-o), or GFP-Arp3-R161A (R161A; Fig. 3.3 p-t) show similar cellular morphology for untransfected, empty vector (only GFP) and GFP-Arp3 (WT) transfected cells, with the majority of cells elaborating long neurites (Fig. 3.3). In contrast, cells expressing GFP-Arp3 (R161A), elaborated few or no neurites and typically had a rounded cell morphology with increased phalloidin staining at the cell cortex (Fig. 3.3 s,t). Untransfected cells did not show any GFP immunoreactivity.

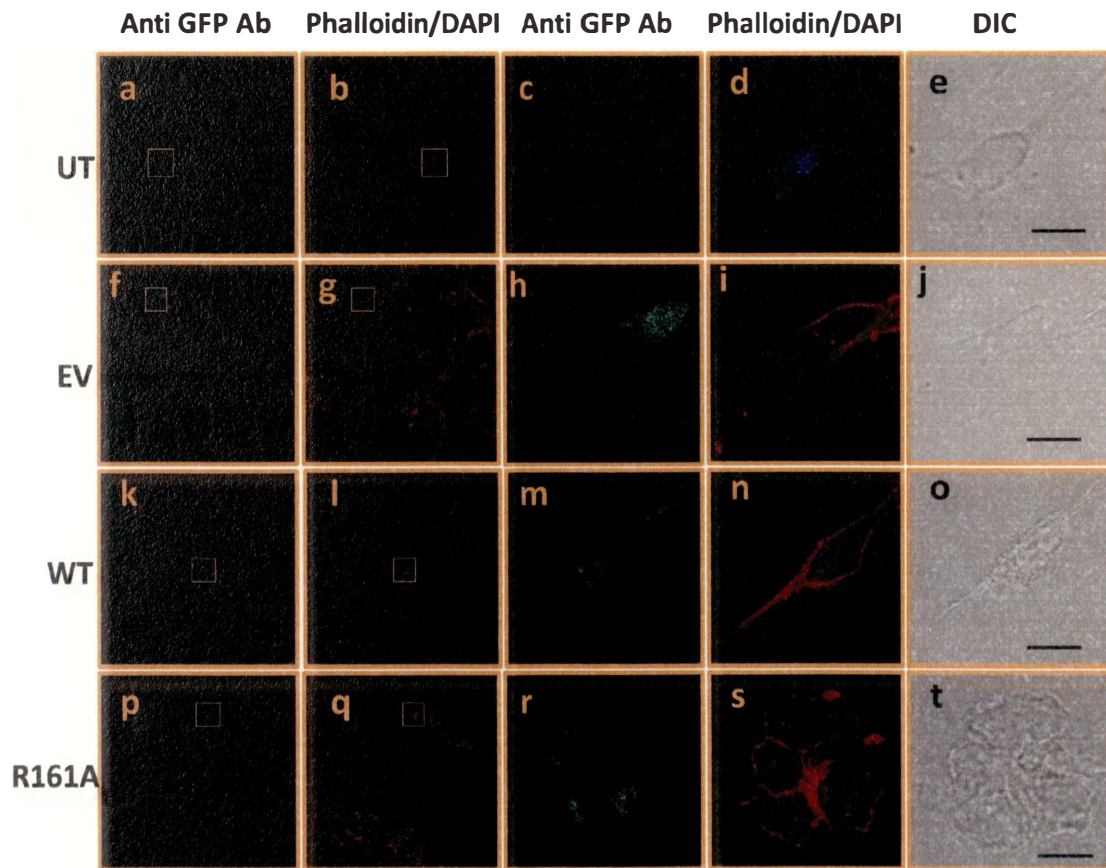


Fig. 3.3. Immunocytochemistry of untransfected cells (a-e) or cells expressing only GFP (f-j), GFP-Arp3(WT) (k-o), or GFP-Arp3-R161A (R161A; p-t) with anti-GFP antibodies (green), Texas-red phalloidin (red) and DAPI (blue) staining (40X). Panels e, j, o, t are DIC images of d, l, n and s, respectively. Panels c, h, m, r are enlarged areas of a, f, k, p, respectively. Panels d, i, n, s are enlarged areas of b, g, l, q, respectively. Scale is 20 μ m.

The mean of the percentage of neurite bearing cells in the R161A group was 23.94% ($p \leq 0.05$) (range 0% - 66.67%), as compared to 96.29% (range 66.67% - 100%), 90.74% (range 50% - 100%) and 91.66% (range 50% - 100%) for the untransfected, empty vector and wild type groups, respectively (fig. 3.4). This might suggest that the

cells expressing the Arp3 mutant (R161A) had decreased neurite initiation. Similarly, the number of neurites per cell (only including cells with neurites) was significantly decreased in cells expressing Arp3-R161A, with a mean of 1.40 (range 1 to 2; $p \leq 0.05$), as compared to the mean of 1.68 (range 1 to 3), 1.96 (range 1 to 3) or 2.15 (range 1 to 4) for the wild-type, empty vector or untransfected groups respectively (fig. 3.5).

Additionally, the number of branches per neurite in cells expressing Arp3-R161A was 0.104 ($p \leq 0.05$), as compared to means of 0.85 in cells expressing wild-type Arp3, as well as untransfected and empty vector, suggesting that any neurite initiated from cells with mutant Arp3 might have a decreased tendency to branch (fig. 3.6). The neurite length per cell was also significantly decreased in cells expressing Arp3-R161A, with a mean of 35.05 microns ($p \leq 0.05$), as compared to means of 100.47, 78.57 and 74.51 for the untransfected, empty vector and wild-type groups, respectively (fig. 3.7). The longest neurite per cell was significantly decreased in cells expressing Arp3-R161A, with a mean of 32.03 microns ($p \leq 0.05$), as compared to a mean of 75.4 microns for untransfected cells (fig. 3.8).

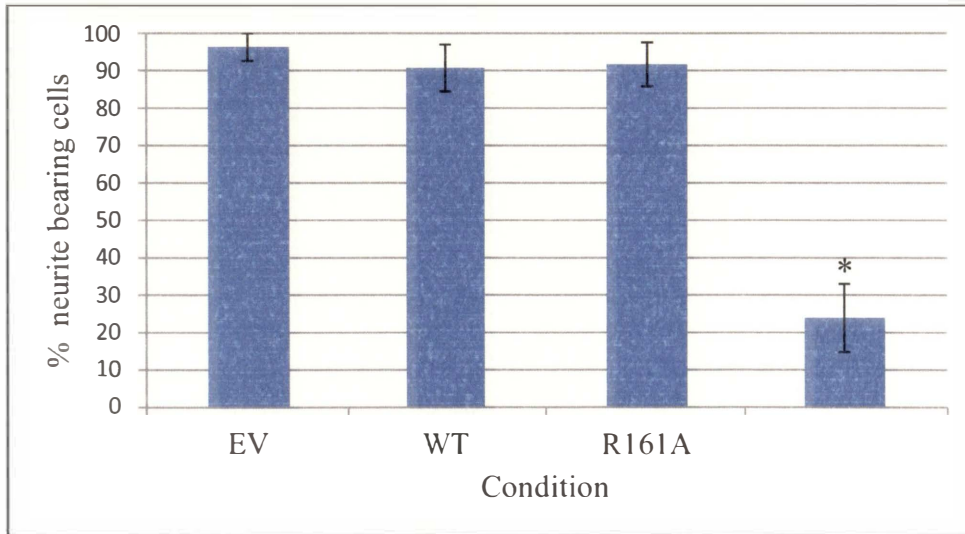


Fig. 3.4. Quantification of the percentage of neurite bearing cells in different treatment groups. Data are means \pm SEM for $n = 9$. Asterisk indicates significant difference from all other groups at $p \leq 0.05$ (ANOVA with LSD post-hoc).

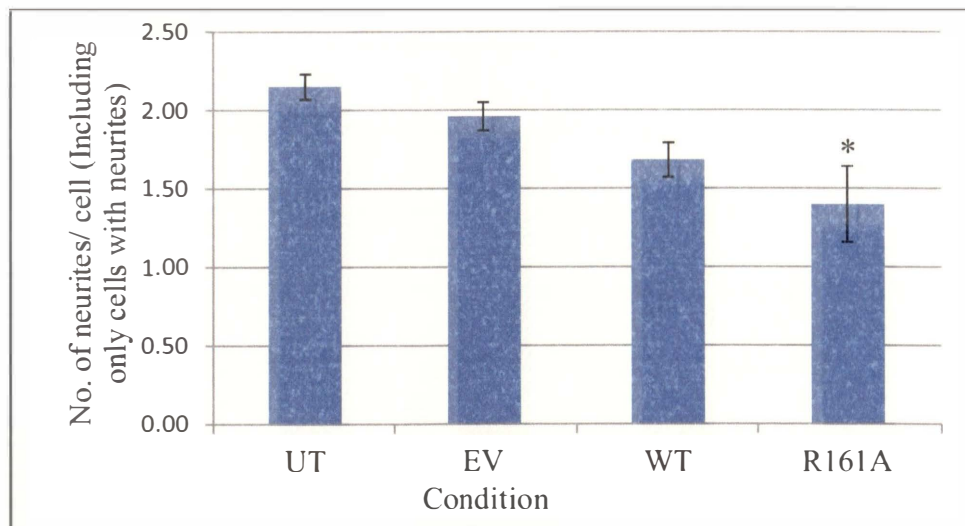


Fig. 3.5. Quantification of the number of neurites per cell in different treatment groups (including only cells with neurites). Data are means \pm SEM for $n = 9$. Asterisk indicates significant difference from all other groups at $p < 0.05$ (ANOVA with LSD post-hoc).

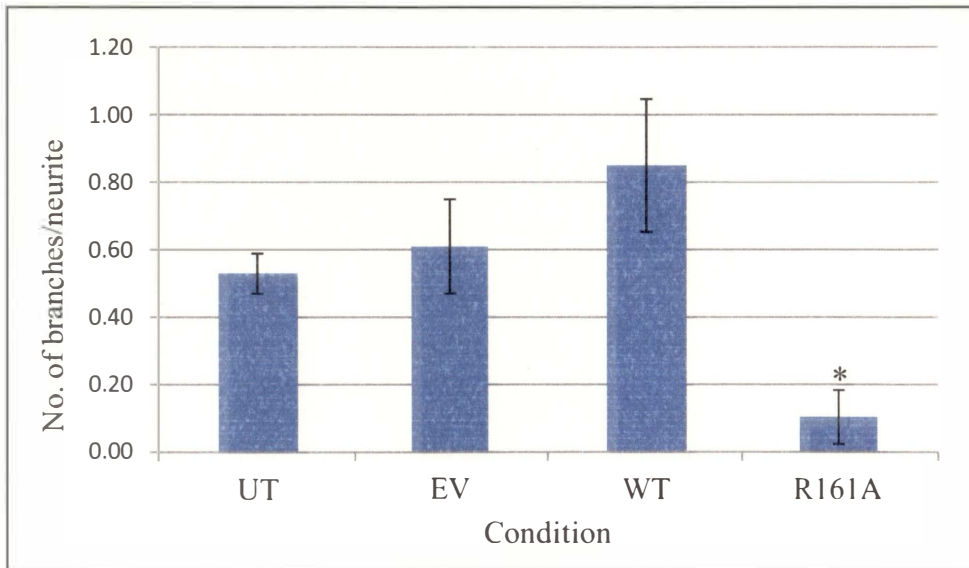


Fig. 3.6. Quantification of the number of branches per neurite in different treatment groups. Data are means \pm SEM for $n = 9$. Asterisk indicates significant difference from all other groups at $p \leq 0.05$ (ANOVA with LSD post-hoc).

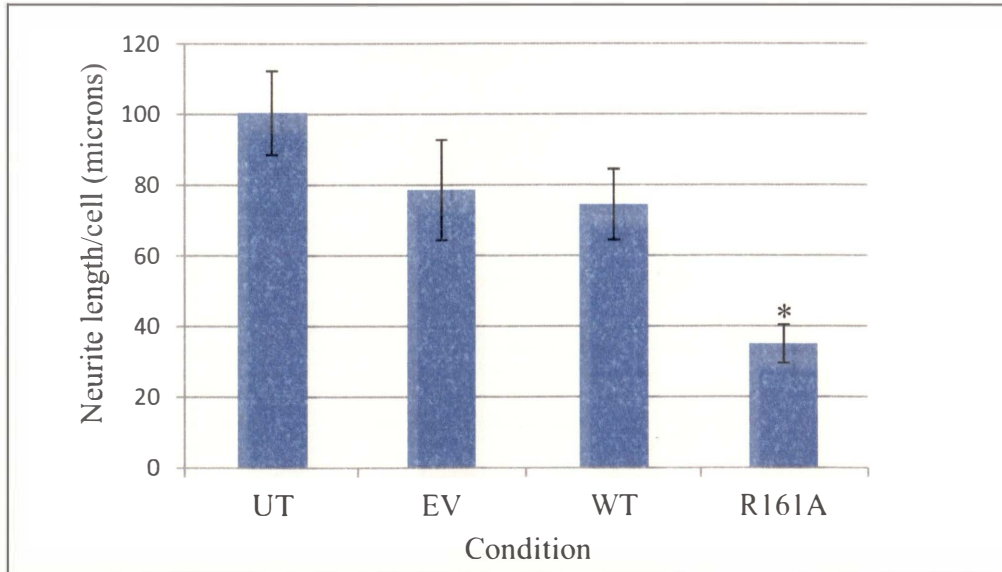


Fig. 3.7. Quantification of the neurite length per cell in different treatment groups. Data are means \pm SEM for $n = 9$. Asterisk indicates significant difference from all other groups at $p \leq 0.05$ (ANOVA with LSD post-hoc).

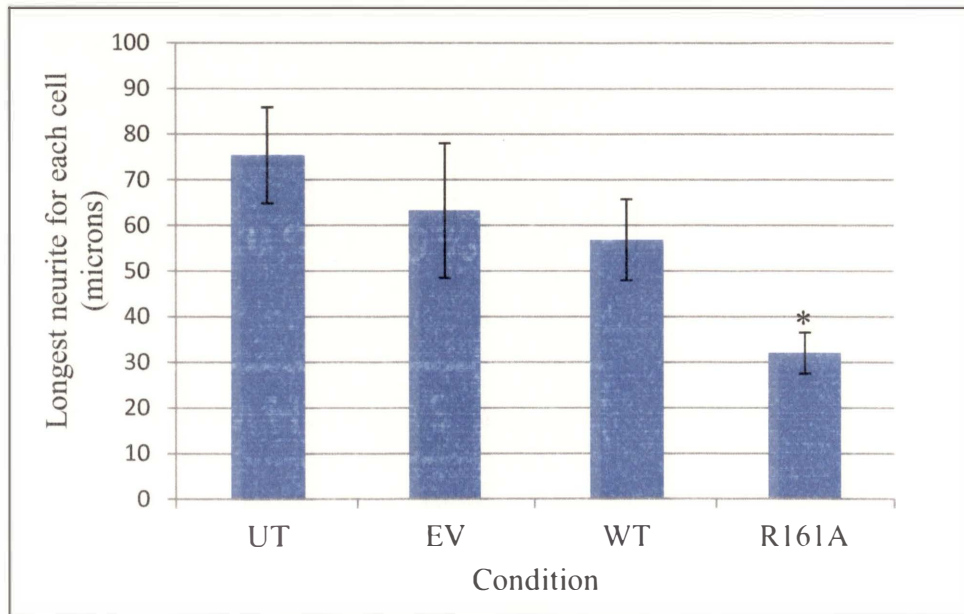


Fig. 3.8. Quantification of the longest neurite per cell in different treatment groups. Data are means \pm SEM for $n = 9$. Asterisk indicates significant difference from UT at $p \leq 0.05$ (ANOVA with LSD post-hoc).

Expression of Arp3-R161A increases lamellipodial actin filament content.

The data presented above show that expressing Arp3-R161A decreases neurite outgrowth, but that this construct can still participate in the Arp2/3 complex. Therefore, we next determined how expressing Arp3-R161A affects the production of actin filament content in lamellipodia. Fig. 3.9 shows the immunocytochemical images of untransfected cells (a-c) and cells transfected with GFP (d-f), GFP-Arp3 (WT; g-i), or GFP-Arp3-R161A (R161A; j-l). Comparison of the Arp3 mutant-expressing cells (Fig. 3.9 k) to those with the in the other treatment groups (Fig. 3.9 b,e,h) indicates a higher cortical phalloidin intensity around cell bodies, suggesting increased actin filament content. Images m, n and o in Fig. 3.9 provide a same field comparison of an untransfected cell

and a cell expressing Arp3-R161A. The cell expressing GFP-Arp3-R161A (green) did not elaborate neurites and demonstrates increased phalloidin staining compared to the untransfected cell, which has typical morphology and a long neurite. The cell body phalloidin fluorescence intensity was increased in cells expressing Arp3-R161A, with a mean of 24.64 arbitrary units ($p \leq 0.05$), as compared to means of 18.52, 17.01 and 17.98 arbitrary units for the untransfected, empty vector and wild-type, respectively (fig.3.10).

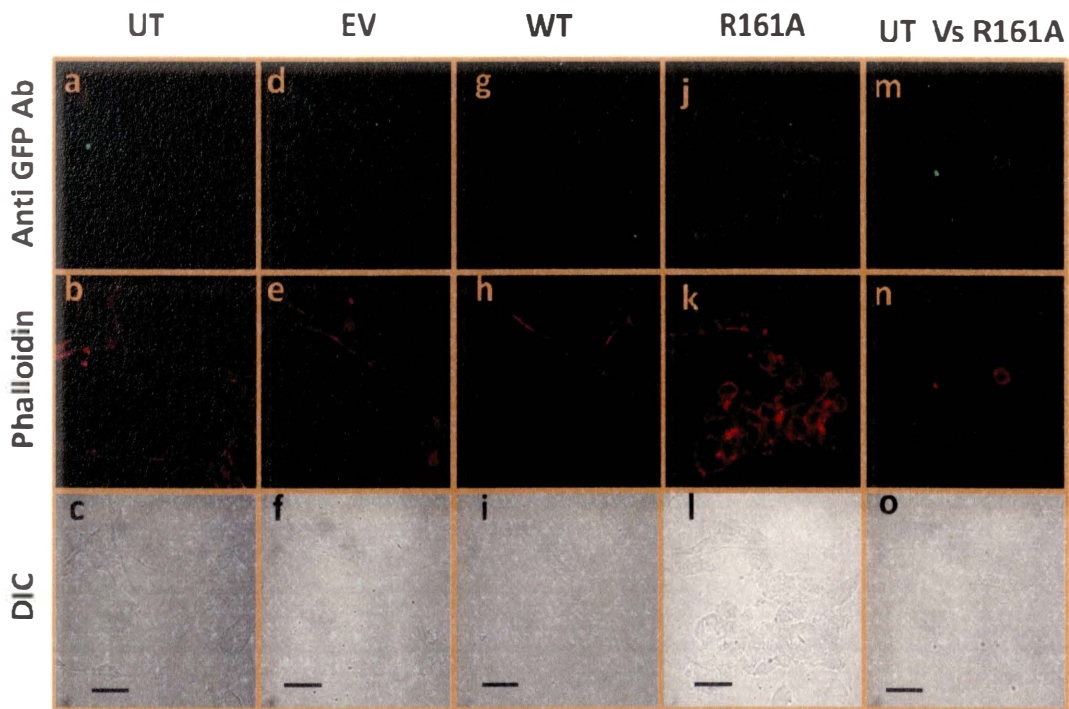


Fig. 3.9. Immunocytochemistry of untransfected cells (a-c) or cell transfected with GFP (d-f), GFP-Arp3(WT; g-i), or GFP-Arp3-R161A (R161A; j-l) with anti-GFP antibodies (a,d,g,j,m; green) along with phalloidin (b,e,h,k,n; red) staining (100X). Panels m-o show a same field comparison of an untransfected cell to a GFP-Arp3-R161A transfected cell immunostained with anti-GFP antibodies (m; green) and stained with phalloidin (n; red) (100X). Scale is 40 μ m.

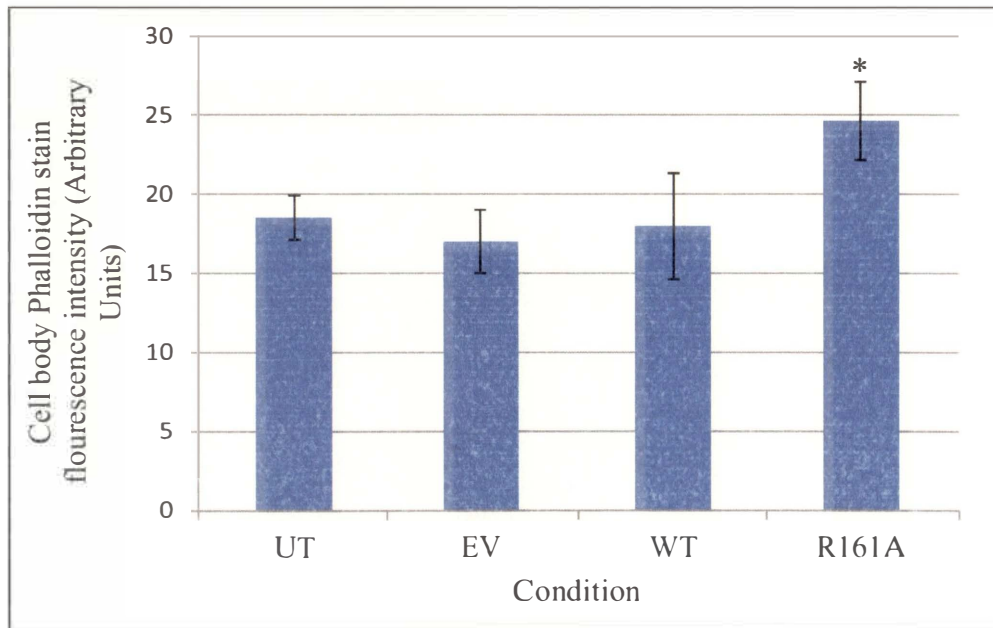


Fig. 3.10. Quantification of cell body phalloidin stain fluorescence intensity in different treatment groups. Data are means \pm SEM for $n = 9$. Asterisk indicates significant difference from all groups at $p \leq 0.05$ (ANOVA with LSD post-hoc).

It was difficult to compare the growth cone lamellipodial phalloidin fluorescence intensity between the different treatment groups due to the decreased number of growth cones in cells expressing Arp3-R161A. An estimate was made by measuring the phalloidin intensity of the lamellipodial regions which showed an increase in the intensity in wild-type cells, perhaps due to overexpression of Arp3. However, this decreased in the R161A group, though it was still high as compared to the untransfected and empty

vector groups (table 3.1). The difference in the intensity was significant ($p \leq 0.05$) in WT as compared to UT or EV.

Table.3.1. Quantification of lamellipodial phalloidin fluorescence intensity in different treatment groups.

Condition	Lamellipodia Phalloidin Stain Fluorescence Intensity (Arbitrary units \pm SEM)
UT	12.13 \pm 1.82 (n = 14)
EV	10.15 \pm 1.93 (n = 8)
WT	27.38 \pm 8.61 (n = 10)
R161A	19.92 \pm 9.96 (n = 3)

DISCUSSION

In this work, we have shown that an R161A point mutation in Arp3 decreases several measure of neurite outgrowth in B35 neuroblastoma cells, including initiation, elongation and branching. Interestingly, Arp3-R161A expression increased cortical actin filament accumulation and the mutant Arp3 was still capable of interacting with Arp2. Furthermore, cells expressing Arp3-R161A have Arp2/3 complexes that interact with

activating WAVE1. These results seem somewhat disparate because it would appear that Arp3-R161A can form a stable Arp2/3 complex, which can interact with its activator; however, expression of the mutated Arp3 results in dramatic decreases in neurite outgrowth. Our results validate those from computational biology simulations suggesting that Arp3 R161 is an important contributor to the Arp2:Arp3 interface and that mutating this residue has profound effects on cellular morphology and lamellipodial actin filament structure. We interpret the results reported herein to suggest that mutating R161 confers an activated form to the Arp2/3 complex, with overexpression of this resulting in excess accumulation of actin to decrease neurite outgrowth.

Several studies suggest that lamellipodia formation and cell motility require Arp2/3 mediated nucleation and polymerization within a narrow, optimal range. Moulding et al. (2007), suggest that cellular processes may be disrupted by increased actin branching and polymerization. In this work, the actin content quantification for the lamellipodia showed an increase in the wild-type and R161A, although it was lower in R161A as compared to wild-type. This may be a consequence of the lack of neurite formation in cells expressing Arp3-R161A. Mutant Arp3 has been reported as one of the major contributors to the abnormal actin assembly in rats with focal and segmental glomerulosclerosis (FSGC; Akiyama et al., 2008). Through mutation of the nucleotide binding sites in Arp2 and Arp3, Martin et al. (2005), showed that ATP binding to both Arp2 and Arp3 is important for the nucleation by Arp2/3 complex. In our computational simulation experiments, mutating R161 of Arp3 was predicted to place the Arp2/3

complex in a closed, active conformation, a function postulated to be attributable to binding of ATP in the nucleotide binding cleft of Arp3.

In this project, the effect of R161A on neurite outgrowth and the interaction between WAVE1 and Arp2/3 complex could give some valuable clues regarding the importance of Arp3 in actin dynamics. Co-IP results suggest that the amounts of WAVE1 binding to Arp2 in the untransfected, empty vector, wild-type and mutant groups are not different. At the same time, one cannot dismiss the idea that WAVE1 is interacting with the Arp2/GFP-Arp3 complex in the wild-type and R161A groups considering the fact that Arp2 is binding to both GFP-Arp3 and GFP-Arp3-R161A.

Although the co-IP studies suggested that the amount of interaction between WAVE1 and Arp2/3 complex was not affected after R161A mutation, immunocytochemistry and confocal imaging studies clearly showed that the cells transfected with Arp3 R161A have poor initiation and growth of neurites. These results seem to contradict the immunoprecipitation results. Thus, it would be expected that the mutation would either have little effect on the morphology of the cells, or that expression of Arp3-R161A would increase neurite outgrowth. Since the actin filament branching is dependent on the affinity of Arp2/3 complex (Goley et al., 2010), it is possible that the mutation in Arp3, irrespective of the interaction of Arp2/3 complex with WAVE1, affected the actin branching process because of change in the affinity of Arp2/3 complex, resulting in the decrease in neurite outgrowth. On the other hand, proteins that directly

help in Arp2/3 complex-mediated actin polymerization and branching facilitate lamellipodial protrusion (e.g. cortactin; Bryce et al., 2005; Siton et al., 2011).

Together, we interpret the data reported here to suggest that the R161A mutation in Arp3 increases efficiency of the Arp2/3 complex for nucleation and actin polymerization. According to D'Agostino et al. (2005), Arp2 helps in the nucleation process. In the same year, it was also shown that nucleotide binding to Arp3 is more important nucleotide binding to Arp2 for proper nucleation activity of the Arp2/3 complex (Martin et al., 2005). The C-domain of WAVE1 brings Arp2 and actin together in the Arp2/3 nucleation process (Chereau et al., 2005). At the same time Wiskott Aldrich Syndrome protein (WASP), a protein similar to WAVE1, has been shown to bivalently bind with Arp2 and Arp3 (Kiselar et al., 2007). Since the amount of WAVE1 interacting with the Arp2/3 complex within the cells was not very different, it is possible that the R161A mutation in Arp3 simply increased or prolonged the activity of Arp2/3 complex or changed its functional structure to an independent activated state by changing the quaternary conformation, thereby enhancing the nucleating capacity of Arp2/3 complex without affecting the WAVE1-Arp2/3 complex interaction. Thus, instead of deactivating the Arp2/3 complex, R161A might have permanently activated the Arp2/3 complex, perhaps eliminating the need for intermediate proteins. This might be the reason for an increase in the actin polymerization and content. A detailed understanding might give us important clues towards manipulating actin nucleation to facilitate recovery from CNS injuries.

CHAPTER IV

FURTHER DISCUSSION

The Discussion sections in Chapters II and III analyze the results from each chapter. However, these analyses do not delve into implications for axon growth in development or regeneration following damage. Here, we elaborate on these aspects of this project.

Appropriate axon extension is necessary for proper development of the nervous system and for successful regeneration following nervous system damage. Axon growth is an intricate process that requires an axon to navigate through a complex environment and then to establish synaptic connections with appropriate targets. Unfortunately, there is little axon extension following damage to the central nervous system (CNS), due in large part to the presence of inhibitors of axon extension. Since axon extension in regeneration is thought to recapitulate developmental axon growth, we need to understand the basics of the axon growth mechanisms.

Axon growth is mediated through interaction of its extending tip, an expanded sensory motile structure called the growth cone (Baas et al., 2001). Growth cone filopodia are finger-like extensions that sample the environment and determine a permissive direction for growth cone advance. However, growth cone advance is thought

to occur primarily through expansion of lamellipodia toward permissive areas. In this work, we investigated mechanisms of growth cone lamellipodial expansion. In particular, lamellipodial expansion occurs through branching actin nucleation and polymerization, resulting in a meshwork of actin filaments within the lamellipodium. This process is controlled by the action of the Arp2/3 complex that binds to the sides of existing actin filaments. The Arp2/3 complex is composed of two actin-like proteins, Arp2 and Arp3, associated with five accessory proteins, ARPC1-5. The Arp2/3 complex is activated through binding of a Wiskott-Aldrich protein, such as WAVE1. The goal of this project was to determine the amino acid residues contributing to the interface between Arp2 and Arp3 and to determine the effects of manipulating the most important of these residues. Using computational biology simulations, we identified arginine 161 (R161) of Arp3 as the most important contributor to the interface. Since it is difficult to mutate endogenous Arp3, we created mammalian expression vectors containing wild-type (WT) Arp3 or Arp3 with R161 mutated to alanine (R161A) and transfected B35 neuroblastoma cells with these constructs to determine the effect of mutating Arp3 R161 on actin nucleation, polymerization and lamellipodial expansion..

Transfection of cells with Arp3-R161A decreased neurite initiation, elongation and branching as compared to cells expression the WT construct. Additionally, Arp3-R161A increased the cellular actin filament content and actin polymerization rate. The mechanisms leading to decreased neurite outgrowth in spite of the increased actin polymerization are not clear, but may be related to an optimal level of branching

polymerization for lamellipodial expansion. Several studies highlight the potential for intricate regulation of Arp2/3 activation. For instance, decreasing the amount of Arp2/3 results in decreased actin branching and polymerization, leading to decreased cellular migration (To et al., 2010), while Arp2 suppression through mutation enhances the nucleating function of Arp2/3 complex (Martin et al., 2005). Our data with cells expressing Arp3-R161A may indicate that the mutation placed the Arp2/3 complex in a permanent active state. One might deduce that activated Arp2/3 should enhance lamellipodia formation and growth cone extension. However, we found that polymerization increased, but neurite outgrowth decreased when Arp3-R161A was expressed, perhaps indicating that too much actin polymerization may impede neurite extension. In support of this idea, proteins that decrease actin filament depolymerization, decrease cell motility (Knecht et al., 2010).

In other systems, electron microscopic studies indicate that actin filament branches formed at the periphery, leading to an accumulation of filaments to result in bundling to form filopodia (Korobova et al., 2008). Since we do not observe growth cone or filopodia formation in cells expressing Arp3-R161A, expressing the mutant Arp3 might be actively inhibiting the actin filament bundling. Another possibility is that expressing Arp3-R161A increases actin polymerization leading to formation of an inappropriate meshwork at the periphery that does not allow organization of actin filaments into bundles of linear filaments needed for neuritogenesis. In either case,

filopodia initiation would be hindered, growth cone formation prevented and neurite growth inhibited.

In addition, our results suggest that Arp2/3 interaction with nucleators, like the Wiskott-aldrich proteins, may not be completely normal. While we find that the Arp2/3 complex can still interact with WAVE1, our studies do not determine if this interaction is still necessary for actin filament meshwork formation. Thus, additional studies investigating the interaction of WAVE1 with Arp2/3 complex and that of Arp3 with Arp2 after the mutation needs to be conducted. It is generally thought that WAVE1 brings Arp3 and Arp2 into a close, active conformation for Arp2/3 complex activation and actin branch nucleation (Robinson et al., 2001). It will be interesting to know if the R161A mutation omitted the need for this step to activate Arp2/3. According to Robinson and colleagues (2001), the Arp3-ARPC2-ARPC3 group and the Arp2-ARPC1-ARPC4-ARPC5 group needs a 20° rotation towards each other for activating nucleation (Robinson et al., 2001). If R161A increased the affinity of Arp2 and Arp3 making it difficult for the two subunits to return to a more open, inactive conformation after activation, it should negate the need for WAVE1 interaction with the complex. In addition, while Arp2/3 is generally thought to work at the sides of existing filaments, some authors support the idea of “barbed end branching” (Pantolini et al., 2000). According to this theory, the activated Arp2/3 complex competes with capping proteins and binds to the barbed end of the filament to produce branching. This leads to a simultaneous growth enhancement of the original and the new branched filament (Falet et

al., 2002). If this is the case, then it is possible that Arp3-R161A increased the affinity of the Arp2/3 complex for the barbed actin filaments, making it more efficient than its competitor capping proteins. Lastly, hydrolysis of bound ATP is needed for Arp2/3 complex activation (Dayel et al., 2001). If expressing Arp3-R161A has negated the need for nucleotide hydrolysis, the Arp2/3 complex in an activated conformation could function in the absence of WAVE1 activation. Answering these questions may lead to a better understanding of the function of the Arp2/3 complex.

Finally, expressing Arp3-R161A may lead to an over-abundance of actin polymerization, preventing growth cone extension. It has been demonstrated that areas of high actin density do not give rise to filopodia and correspond to expanded lamellipodia (Verkhovskiy et al., 2003). According to Verkhovskiy et al. (2003), any activator of Arp2/3 complex gives rise to the high density areas. This is in contrast to the Korobova & Svitkina model, which suggests that areas of increased actin filament meshwork formation lead to development of filopodia (Korobova et al., 2008). Thus, it may be that beyond a threshold of actin density, filopodia formation is prevented. Our data indicate that there is an increase in the actin polymerization *in vitro* from extracts of cells expressing Arp3-R161A and in the accumulation of cortical actin content in intact cells. The findings suggest the possibility that the increased cellular actin content, probably due to increased activity of Arp2/3 complex, lead to an inappropriate actin filament meshwork formation. This, in turn, might have prevented filopodia protrusion and growth cone elongation. An electron microscopic study of the structural effects of increased actin

polymerization and branching on the filopodia initiation would confirm further, the actual mechanism taking place at the periphery of the cells and at the neurite branch-points.

To summarize, having an arginine at position 161 is important for an Arp2-Arp3 interface that facilitates appropriate levels of actin nucleation and polymerization. R161A mutation of Arp3 possibly increases the capacity or shifts the equilibrium toward the activated state of Arp2/3 without affecting its interaction with WAVE1, leading to an increase in actin nucleation and polymerization. This forms a high actin filament density along the plasma membranes of B35 neuroblastoma cells, which may prevent filopodia initiation and growth cone elongation. In a sense, this dense network formation prevents organization of actin filaments into proper functional cellular processes. Further protein interaction and electron microscopic studies of cells with R161A mutation are needed for a better understanding the role of R161 in regulating the Arp2-Arp3 interface and actin filament meshwork formation. Understanding these process will improve our understanding of the molecular mechanisms regulating axon growth and may identify novel therapeutic targets to enhance regeneration following nervous system damage.

REFERENCES

- Akiyama K, Morita H, Suetsugu S, Kuraba S, Numata Y, Yamamoto Y, Inui K, Ideura T, Wakisaka N, Nakano K, Oniki H, Takenawa T, Matsuyama M, Yoshimura A (2008) Actin -related protein 3 (Arp3) is mutated in proteinuric BUF/Mna rats. *Mammalian Genome* 19(1):41-50.
- Alto LT, Havton LA, Conner JM, Hollis II EM, Blesch A, Tuszynski MH (2009) Chemotropic guidance facilitates axonal regeneration and synapse formation after spinal cord injury. *Nature Neuroscience* 12(9):1106-1113.
- Aspenstrom P (1999) The Rho GTPases have multiple effects on the actin cytoskeleton. *Experimental Cell Research*, 246:20-25.
- Baas PW, Luo L (2001) Signaling at the growth cone: The scientific progeny of Cajal meet in Madrid. *Neuron*, 32:981-984.
- Beltzner CC, Pollard TD (2003) Identification of functionally important residues of Arp2/3 complex by analysis of homology models from diverse species. *Journal of Molecular Biology* 336:551-565.
- Beltzner CC, Pollard TD (2007) Pathway of actin filament branch formation by Arp2/3 complex. *The Journal of Biological Chemistry* 283:7135-7144.

- Bertani G (1951) Studies on lysogenesis I. The mode of phage liberation by lysogenic *Escherichia coli*. *Journal of Bacteriology* 62:293-300.
- Boczkowska M, Rebowski G, Petoukhov MV, Hayes DB, Svergun DI, Dominguez R (2008) X-ray scattering study of activated Arp2/3 complex with bound actin-WCA. *Structure* 16: 695-704.
- Bompard G, Caron E (2004) Regulation of WASP/WAVE1 proteins: Making a long story short. *The Journal of Cell Biology*, 166 (7):957-962.
- Bryce NS, Clark ES, Leysath JL, Currie JD, Webb DJ, Weaver AM (2005) Cortactin promotes cell motility by enhancing lamellipodial persistence. *Current Biology*, 15:1276–1285.
- Chereau D, Kerff F, Graceffa P, Grabarek Z, Langsetmo K, Dominguez R (2005) Actin-bound structures of Wiskott–Aldrich syndrome protein (WASP)-homology domain 2 and the implications for filament assembly. *Proceedings of the National Academy of Sciences*, 102(46):16644-16649.
- D'Agostino JL, Goode BL (2005) Dissection of Arp2/3 complex actin nucleation mechanism and distinct roles for its nucleation-promoting factors in *Saccharomyces cerevisiae*. *Genetics*, 171:35–47.
- Dayel MJ, Holleran EA, Mullins RD (2001) Arp2/3 complex requires hydrolyzable ATP for nucleation of new actin filaments. *Proceedings of the National Academy of Sciences*, 98:14871–14876.

- DesMarais V, Macaluso F, Condeelis J, Bailly M (2004) Synergistic interaction between the arp2/3 complex and cofilin drives simulated lamellipodia extension. *Journal of Cell Science*, 117(16):3499-3510.
- Dickson B (2001) Rho GTPases in growth cone guidance. *Current Opinion in Neurobiology*, 11: 103-110.
- Dominguez R (2009) Actin filament nucleation and elongation factors- structure-function relationships. *Critical Reviews in Biochemistry and Molecular Biology*, 44(6):351- 366.
- Dou F, Huang L, Yu P, Zhu H, Wang X, Zou J, Lu P, Xu X (2009) Temporospatial expression and cellular localization of oligodendrocyte myelin glycoprotein (OMgp) after traumatic spinal cord injury in adult rats. *Journal of Neurotrauma*, 26:2299-2311.
- Falet H, Hoffmeister KM, Neujahr R, Italiano Jr, JE, Stossel TP, Southwick FS, Hartwig JH (2002) Importance of free actin filament barbed ends for Arp2/3 complex function in platelets and fibroblasts. *Proceedings of the National Academy of Sciences*, 99:16782–16787.
- Garrity P (1999) Signal transduction in axon guidance. *Cell Molecular Life Science*, 55:1407-1415.
- Goldberg D, Foley M, Tang D, Grabham P (2000) Requirement of the Arp2/3 complex and Mena for the stimulation of actin polymerization in growth cones by nerve growth factor. *Journal of Neuroscience Research*, 60, 458-467.

- Goley ED, Rammohan A, Znameroski EA, Firat-Karalar EN, Sept D, Welch MD (2010) An actin-filament-binding interface on the Arp2/3 complex is critical for nucleation and branch stability. *Proceedings of the National Academy of Sciences*, 107(18):8159-8164.
- Hall A (1998) Rho GTPases and the actin cytoskeleton. *Science*, 279:509-514.
- Kiselar JG, Mahaffy R, Pollard TD, Almo SC, Chance MR (2007) Visualizing Arp2/3 complex activation mediated by binding of ATP and WASp using structural mass spectrometry. *Proceedings of the National Academy of Sciences of the United States of America*, 104(5):1552-1557.
- Knecht DA, LaFleur RA, Kahsai AW, Argueta, CE, Beshir AB, Fenteany G (2010) Cucurbitacin I inhibits cell motility by indirectly interfering with actin dynamics. *PLoS*, 5(11):e14039.
- Korobova F, Svitkina T (2008) Arp2/3 complex is important for filopodia formation, growth cone motility, and neuritogenesis in neuronal cells. *Molecular Biology of Cell*, 19:1561-1574.
- Kortemme T, Klm DE, Baker D (2004) Computational alanine scanning of protein-protein interfaces. *Science's Signal Transduction Knowledge Environment*, 219(19):1-8.
- Leung DW, Otomo C, Chory J, Rosen MK (2008) Genetically encoded photoswitching of actin assembly through the Cdc42-Wasp-Arp2/3 complex pathway. *Proceedings of the National Academy of Sciences*, 105(35):12797-12802.

- Lichtarge O, Bourne HR, Cohen FE (1996) An evolutionary trace method defines binding surfaces common to protein families. *Journal of Molecular Biology*, 257:342-358.
- Liu SL, Needham KM, May JR, Nolen BJ (2011) Mechanism of a concentration-dependent switch between activation and inhibition of Arp2/3 complex. *The Journal of Biological Chemistry*, 286(19):17039-17046.
- Lu P, Yang H, Jones LL, Filbin MT, Tuszynski MH (2004). Combinatorial therapy with neurotrophins and cAMP promotes axonal regeneration beyond sites of spinal cord injury. *Journal of Neuroscience*, 24:6402–6409.
- Luo L, Jan L, Jan Y (1996) Small GTPases in axon outgrowth. *Perspectives on Developmental Neurobiology*, 4:199-204.
- Machesky SM, Simon J, Ampe C, Vandekerckhove J, Pollard TD (1994) Purification of a cortical complex containing two unconventional actins from *acanthamoeba* by affinity chromatography on profilin-agarose. *The Journal of Cell Biology*, 127(1):107-115.
- Martin AC, Xu X, Rouiller I, Kaksonen M, Sun Y, Belmont L, Volkmann N, Hanein D, Welch M, Drubin DG (2005) Effects of Arp2 and Arp3 nucleotide-binding pocket mutations on Arp2/3 complex function. *Journal of Cell Biology*, 168(2):315-328.
- Maruyama K, Kurokawa H, Oosawa M, Shimaoka S, Yamamoto H, Ito M, Maruyama K (1990) Beta-actinin is equivalent to Cap Z protein. *Journal of Biological Chemistry*, 265(15):8712-5.

- Meyer G, Feldman E (2002) Signaling mechanisms that regulate actin- based motility processes in the nervous system. *Journal of Neurochemistry*, 83:490- 503.
- Millard TH, Sharp SJ, Machesky LM (2004) Signalling to actin assembly via the WASP (Wiskott–Aldrich syndrome protein)-family proteins and the Arp2/3 complex. *Biochemical Journal*, 380:1– 17.
- Moulding DA, Blundell MP, Spiller DG, White MR, Cory GO, Calle Y, Kempinski H, Sinclair J, Ancliff PJ, Kinnon C, Jones GE, Thrasher AJ (2007) Unregulated actin polymerization by WASp causes defects of mitosis and cytokinesis in X-linked neutropenia. *The Journal of Experimental Medicine*, 204(9):2213-2224.
- Mueller B (1999) Growth cone guidance: First steps towards the deeper understanding. *Annual Review Neuroscience*, 22:351-388.
- Mullins R (2000) How WASP-family proteins and the Arp2/3 complex convert intracellular signals into cytoskeletal structures. *Cell Biology*, 12:91-96.
- Nikolic M (2002) The role of Rho GTPases and associated kinases in regulating neurite outgrowth. *The International Journal of Biochemistry and Cell Biology*, 34:731-745.
- Nolen BJ, Littlefield RS, Pollard TD (2004) Crystal structures of actin-related protein 2/3 complex with bound ATP or ADP. *PNAS*, 101(44):15627-15632.
- Nolen BJ, Pollard TD (2008) Structure and biochemical properties of fission yeast Arp2/3 complex lacking the Arp2 subunit. *Journal of Biological Chemistry*, 283(39):26490-26498.

- Otterbein L, Philip G, Roberto D (2001) The crystal structure of uncomplexed actin in the ADP state. *Science*, 293(5530):708.
- Padrick S, Cheng H, Ismail A, Panchal S, Doolittle L, Kim S, Skehan B, Umetani J, Brautigam C, Leong J, Rosen M (2008) Hierarchical regulation of WASP/WAVE1 proteins. *Molecular Cell*, 32(3):426-438.
- Pantaloni D, Boujemaa R, Didry D, Gounon P, Carlier MF (2000) The Arp2/3 complex branches filament barbed ends: functional antagonism with capping proteins. *Nature Cell Biology*, 2:385–391.
- Pinyol R, Haeckel A, Ritter A, Qualmann B, Kessels MM (2007) Regulation of N-WASP and the Arp2/3 complex by Abp1 controls neuronal morphology. *Plos One*, 2(5)e400:1-15.
- Pollard TD, Borisy GG (2003) Cellular motility driven by assembly and disassembly of actin filaments. *Cell*, 112:453-465.
- Robinson RC, Turbedsky K, Kaiser DA, Marchand JB, Higgs HN, Choe S, Pollard TD (2001) Crystal structure of Arp2/3 complex. *Science*, 294:1679- 1683.
- Rodal A, Sokolova O, Robins D, Daugherty K, Hippenmeyer S, Riezman H, Grigorieff N, Goode B (2005) Conformational changes in the Arp2/3 complex leading to actin nucleation. *Nature Structural and Molecular Biology*, 12:26-31.
- Rouiller I, Xu X, Amann K, Egile C, Nickell S, Nicastró D, Li R, Pollard T, Volkman N, Hanein D (2008) The structural basis of actin filament branching by the Arp2/3 complex. *The Journal of Cell Biology*, 180(5):887-895.

- Schmidt H, Rathjen FG (2010) Signalling mechanisms regulating axonal branching *in vivo*. *Bioessays*, 32:977–985.
- Seifert J (2008) Compartmentalized Rho GTPase activation is associated with effects on actin binding proteins. Published manuscript, Department of Biology, Texas Woman's University, Denton, Texas, USA.
- Shakir MA, Jiang K, Struckhoff EC, Demarco RS, Patel FB, Soto MC, Lundquist EA (2008) The Arp2/3 activators WAVE1 and wasp have distinct genetic interactions with Rac GTPases in *Caenorhabditis elegans* axon guidance. *Genetics*, 179:1957-1971.
- Siton O, Ideses Y, Albeck S, Unger T, Bershadsky AD, Gov NS, Bernheim-Groswasser A (2011) Cortactin releases the brakes in actin- based motility by enhancing WASP-VCA detachment from Arp2/3 branches. *Current Biology*, 21(24):2092-2097.
- Skaper S, Moore S, Walsh F (2001) Cell signaling cascades regulating neuronal growth-promoting and inhibitory cues. *Progress in Neurobiology* 65:593-608.
- Song H, Poo M (2001) The cell biology of neuronal navigation. *Nature Cell Biology*, 3:E81-E88.
- To C, Shilton BH, Di Guglielmo GM (2010) Synthetic triterpenoids target the Arp2/3 complex and inhibit branched actin polymerization. *The Journal of Biological Chemistry*, 285(36):27944-27957.

Verkhovsky AB, Chaga OY, Schaub S, Svitkina TM, Meister JJ, Borisy GG (2003)

Orientational order of the lamellipodial actin network as demonstrated in living motile cells. *Molecular Biology of the Cell*, 14:4667- 4675.

Wegner AM, Nebhan CA, Hu L, Majumdar D, Meier KM, Weaver AM, Webb DJ (2008)

N-Wasp and the Arp2/3 complex are critical regulators of actin in the development of dendritic spines and synapses. *Journal of Biological Chemistry*, 283(23):15920-15920.